

# Exploring senescent chondrocytes during aging: sleeper AGEnts of osteoarthritis

Boone, I.

#### Citation

Boone, I. (2025, October 17). Exploring senescent chondrocytes during aging: sleeper AGEnts of osteoarthritis. Retrieved from https://hdl.handle.net/1887/4273547

Version: Publisher's Version

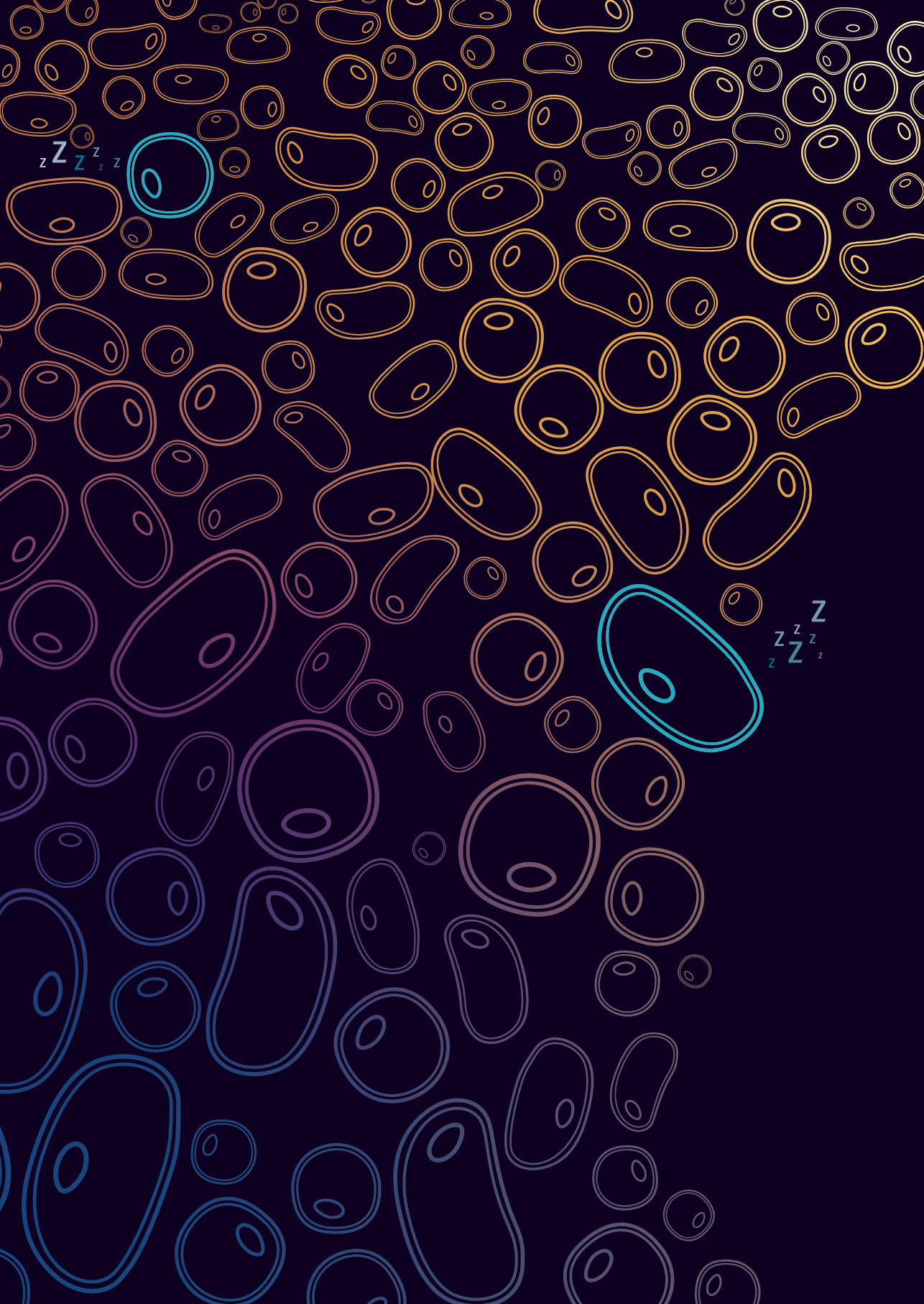
Licence agreement concerning inclusion of doctoral

License: thesis in the Institutional Repository of the University

of Leiden

Downloaded from: <a href="https://hdl.handle.net/1887/4273547">https://hdl.handle.net/1887/4273547</a>

**Note:** To cite this publication please use the final published version (if applicable).





# Identified senescence endotypes in aged cartilage are reflected in the blood metabolome

I. Boone<sup>1</sup>, M. Tuerlings<sup>1</sup>, R. Coutinho De Almeida<sup>1</sup>, J. Lehmann<sup>2</sup>, Y.F.M. Ramos<sup>1</sup>, R.G.H.H. Nelissen<sup>3</sup>, P. Slagboom<sup>1,4</sup>, P.L.J. de Keizer<sup>2,5</sup>, I. Meulenbelt<sup>1\*</sup>

<sup>1</sup>Dept. of Biomedical Data sciences, section Molecular Epidemiology, Leiden University Medical Center, Leiden. The Netherlands

<sup>2</sup>Center for Molecular Medicine, Division of Laboratories, Pharmacy and Biomedical Genetics, University Medical Center Utrecht, Utrecht, The Netherlands

<sup>3</sup>Dept. of Orthopaedics, Leiden University Medical Center, Leiden, The Netherlands

<sup>4</sup>Max Planck Institute for Biology of Aging, Cologne, Germany

<sup>5</sup>Cleara Biotech B.V., Utrecht, The Netherlands

\* Corresponding author

This chapter is based on the article manuscript "Identified senescence endotypes in aged cartilage are reflected in the blood metabolome"

Geroscience 46.2 (2024): 2359-2369. Doi: 10.1007/s11357-023-01001-2

# **Abstract**

Heterogeneous accumulation of senescent cells expressing the senescence-associated secretory phenotype (SASP) affect tissue homeostasis which lead to diseases, such as osteoarthritis (OA). In this study, we set out to characterize heterogeneity of cellular senescence within aged articular cartilage and explored the presence of corresponding metabolic profiles in blood that could function as representative biomarkers. Hereto we set out to perform cluster analyses, using a gene-set of 131 senescence genes (N=57) in a previously established RNA sequencing dataset of aged articular cartilage, and a generated metabolic dataset in overlapping blood samples. Using unsupervised hierarchical clustering and pathway analysis, we identified two robust cellular senescent endotypes. Endotype 1 was enriched for cell proliferating pathways, expressing Forkhead Box Protein O4 (FOXsO4), RB Transcriptional Corepressor Like 2 (RBL2) and Cyclin Dependent Kinase Inhibitor 1B (CDKN1B), the FOXO mediated cell cycle was identified as possible target for endotype 1 patients. Endotype 2 showed enriched inflammation associated pathways, expressed by Interleukin 6 (IL6), Matrix Metallopeptidase (MMP) 1/3 and Vascular Endothelial Growth Factor (VEGF)C and SASP pathways were identified as possible targets for endotype 2 patients. Notably, plasma-based metabolic profiles in overlapping blood samples (N=21), showed two corresponding metabolic clusters in blood. These non-invasive metabolic profiles could function as biomarkers for patient-tailored targeting of senescence in OA.

#### Keywords

Osteoarthritis | Senescence | blood-biomarkers | Endotypes | metabolic blood profiles

# Introduction

Osteoarthritis (OA) is a prevalent, age-related, and painful degenerative disease of joint tissues without curative treatment options 1. Although all joint tissues have been implicated in OA, a hallmark of OA pathophysiology is the progressive degradation of articular cartilage. With the low reparative capacity of chondrocytes, the sole cell type in articular cartilage, important risk factors triggering OA pathophysiology are excessive mechanical stress, and age 2.3. In this respect, we have previously studied downstream effects of hyper physiological mechanical stress applied to aged human ex vivo osteochondral explants and highlighted enrichment of GO-term "cellular senescence". Senescence is one of the hallmarks of aging and is brought about by pro-survival strategies that cells use to avoid apoptosis upon cellular stress 3. Nonetheless, such strategies in postmitotic cells, such as chondrocytes in articular cartilage, are likely different from the classical cellular senescence process where cells go into irreversible cell-cycle arrest, marked by permanent CDK inhibitor as p21<sup>Cip1</sup> or p16<sup>ink4a 4-6</sup>. Therefore, senescence is more recently described as a complex process involving metabolic morphologic transformation of cells in response to cellular stressors, such as oxidative or mechanical stress 4,7. Notably, senescent cells express a harmful pro-inflammatory profile such as interleukin (IL)1B, IL6, matrix metalloproteinases (MMP) family member-13 and tumor necrosis factor A (TNFA), known as the senescence associated secretory phenotype (SASP), that drives neighboring cells to also go into senescence<sup>5,8</sup>. More specific, these SASP markers are well known to have an adverse effect on chondrocyte health, likely affecting propensity of chondrocytes to enter a disease OA like state 6.9. Other lines of evidence imply the involvement of cellular senescence during OA pathophysiology such as the presence of senescence markers in OA tissue (e.g.p16<sup>INK4A</sup> and p21) <sup>4-6</sup>, age related increase of senescence-associated beta galactosidase (SA-B-gal) activity, and increased presence of SASP markers in OA cartilage 6,9,10. In mice, implantation of senescent cells into cartilage induced an OA-like environment, marked by the degeneration of cartilage and osteophyte formation 11.

The field has in recent years developed multiple drugs to target senescent cells either by, selectively killing senescent cells (senolytics), or modifying their behavior (senomorphics) <sup>12</sup>. Due to the lack of disease modifying OA drugs <sup>13</sup> and the putative role of senescent cells in OA pathophysiology, these drugs have been suggested as a therapeutic option for OA <sup>14</sup>. Nonetheless, prior to such a therapeutic avenue, insight into the diversity of cellular senescence in aged articular cartilage is required <sup>15</sup>. Moreover, to allow translation of such knowledge into clinical practice, associated non-invasive biomarkers of the diversity must be developed. For that matter, metabolic features in the circulation are considered potent candidates, as they play a vital role in predicting vulnerability and frailty with aging <sup>16-18</sup>.

Together, we here set out to characterize diversity of senescence in aged articular cartilage by analyzing a custom senescence associated gene-set across our previously assessed mRNA-sequencing dataset <sup>19</sup>. Moreover, to allow translation to the clinic we studied the potency of metabolic features in blood as corresponding biomarkers of this diversity in aged articular cartilage.

# **Method**

#### Sample description

Preserved (macroscopically healthy) cartilage (N=57) as well as blood samples (N=123) were obtained from patients who underwent joint replacement surgery due to end-stage OA (Research Arthritis and Articular Cartilage, RAAK study). In the current study, 57 preserved cartilage samples were used (Supplementary table 1). From the 57 samples, there was an overlap of 21 patients of which preserved cartilage and blood data was available (Figure 1). A senescence dataset was created for the current study, consisting of 155 senescence genes obtained from literature (Supplementary table 2), from which 24 senescence genes were not expressed in OA cartilage (Supplementary table 2). Therefore, further analysis was performed on 131 senescence genes expressed in cartilage.

#### **RNA** sequencing

mRNA sequencing of the preserved and lesioned cartilage samples was previously achieved on the Illumina HiSeq 2000, HiSeq 4000 and HiSeq X ten. Quality control was performed using an in-house pipeline as described previously <sup>7,19</sup>. In short, the data was corrected for batch effects and subsequently normalized and transformed using the Variance Stabilizing Transform (VST) method.

#### Unsupervised hierarchical clustering

To avoid looking at the end-stage OA phenotype, further analysis was performed on the 57 preserved cartilage samples and 131 expressed senescence genes. Unsupervised hierarchical clustering (ComplexHeatmap, v2.8.0 R package<sup>20</sup>) was performed on the normalized mRNA-seq data to identify different endotypes (clusters) of genes present in preserved cartilage (Figure 1). Hierarchical clustering was performed on the expression levels of the 131 senescence genes, using Spearman's correlation as distance and complete clustering as method. Expression levels of genes selected for endotypes 1 and 2 were validated in preserved cartilage tissue (N=8-13, due to quality control, Figure 1) using quantitative reverse transcription PCR (RT-qPCR) adjusting for housekeeping genes POU Class 6 homeobox 1 (*POU6F1*) and HECT Domain E3 Ubiquitin Protein Ligase 3 (*HECTD3*).

### Differential expression analysis

Differentially expression (DE) analysis was performed on the endotypes revealed with unsupervised hierarchical clustering present in preserved cartilage samples from the RAAK study <sup>19</sup>. DE analysis was performed as described previously <sup>21</sup>. In short, data was batch corrected and subsequently normalized and log2-transformed. P-values were Benjamini-Hochberg multiple testing corrected and <0.05 was considered significant. Endotype 1 was used as baseline. All genes with a negative foldchange and FDR<0.05 were retained to endotype 1 (Supplementary table 3) and genes with a significant positive foldchange were retained to endotype 2 (Supplementary table 4). A protein-protein interaction network was made using STRING v12.0 <sup>22</sup> with settings set to high confidence (0.700) and query proteins only.

## Pathway analysis

Pathway analysis was performed per endotype using the differentially expressed genes (Figure 1). The pathway analysis was performed with DAVID v2021  $^{23}$  with a background correction for genes

expressed in cartilage, selecting for GOTERM\_BP\_DIRECT, GOTERM\_CC\_DIRECT, GOTERM\_MF\_DIRECT, KEGG pathway and REACTOME pathway. Subsequently, unique pathways (FDR significant, FDR<0.05, and not expressed in the other endotype) pathways were selected.

#### **Drug-gene interaction**

Drug-gene interactions were found with the Drug Gene Interaction Database (DGIdb, v4.2.0 <sup>24</sup>, filtering on approved drugs) using the 10 most significant differentially expressed genes for endotype 1 and -2. Further network analysis was performed using STITCH v5.0 <sup>25</sup> with high confidence (0.700).

#### Metabolomic analysis

EDTA plasma samples (N=123) were analyzed by Nightingale (Nightingale Ltd, Helsinki, Finland). This 1H-NMR technique resulted in 249 metabolic trait measurements. Quality control was performed; metabolic biomarkers with more than 5 below detection limit were removed from further analysis and PCA analysis was performed to check for outliers (Supplementary Figure 3). To limit the change of overfitting, 63 underived and independent metabolomic measurements were used for further analysis <sup>17</sup>. Data of 63 metabolic biomarkers and 123 patients was scaled using the scale function for the base package of R. The data of 21 patients (overlapping with cartilage mRNA, Figure 1) was subsequently clustered using Spearman's correlation distance and complete clustering using ComplexHeatmap v.2.8.0 R package <sup>20</sup>. Significant metabolic biomarkers between the metabolic endotypes were determined with a generalized equation estimate model using geese of geepack v.1.3.3 R package <sup>26</sup> with formula: Metabolic biomarker ~ Metabolic Endotype + Age + Sex + BMI. Subsequently, the data of 63 metabolic biomarkers and 123 patients was clustered using Spearman's correlation distance and complete clustering using ComplexHeatmap v.2.8.0 R package.

# **Results**

# Aged human articular cartilage reveals a senescence signature

To investigate the role of senescence in aged articular cartilage, expression levels of 155 senescence-associated genes (Supplementary table 2) were analyzed in a previously assessed RNA sequencing dataset of N=57 macroscopically normal (preserved) articular cartilage of patients undergoing a joint replacement surgery due OA (The RAAK study, Supplementary table 1) <sup>19</sup>. *In silico* exploration of the 155 senescence associated genes, showed 131 genes that had detectable expression levels (Supplementary table 2). As shown in Supplementary table 2, While the widely acknowledged senescent marker cyclin dependent kinase inhibitor (*CDKN*)2A, encoding p16INK4A, was lowly expressed in aged articular cartilage while *CDKN1A*, encoding p21, was highly expressed in aged articular cartilage. Amongst the highest expressed senescence associated genes were fibronectin (*FN1*), TIMP Metallopeptidase Inhibitor (*TIMP*)1, Insulin Like Growth Factor Binding Protein (*IGFBP*)5 and *VEGFA*. On the other hand among the factors marking the SASP, we recognized insulin like growth factor (IGF) pathway, *IGFBP2* and 3 and matrix metalloproteinases family members, *MMP3* and *MMP13* as being highly expressed (Upper quartiles 3 and 4, Supplementary table 2) in aged articular cartilage.

# Unsupervised hierarchical clustering of the senescence signature in aged human articular cartilage

To identify diversity of senescence processes in aged human articular cartilage, unsupervised hierarchical clustering was performed on RNA expression levels of the 131 senescence associated genes (Figure 1). Two distinct endotypes were identified, hereafter denoted as cartilage senescence endotype 1 and endotype 2 (Figure 2A). To characterize the molecular senescent landscape between the endotypes further, differential gene expression analysis was performed. In total, 75 differential genes were identified (FDR < 0.05) with 24 genes marking endotype 1 related senescence (higher expressed in endotype 1, Supplementary table 3) and 51 genes marking endotype 2 related senescence (higher expressed in endotype 2, Supplementary table 4).

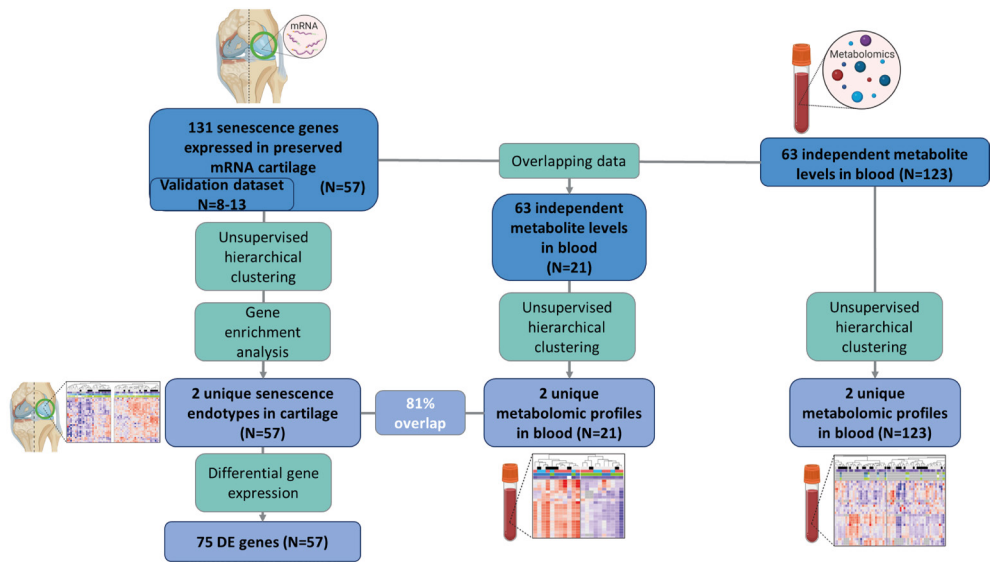


Figure 1 - Study approach. 131 senescence genes were characterized in preserved cartilage (N=57). Unsupervised hierarchical clustering and gene enrichment analysis was performed to find senescence endotypes in human aged cartilage. To find descriptive genes for the clusters, differential gene expression analysis was used. Metabolic blood profiles were extracted using unsupervised hierarchical clustering on metabolite levels in blood in an overlapping dataset with preserved cartilage (N=21). Overlap between the cartilage endotypes and metabolic blood profiles was assessed. Unsupervised hierarchical clustering was performed on the total metabolite dataset (N=123). Created with bioRender.com

### Characteristics of senescence endotype 1 in aged articular cartilage

Figure 3A shows the protein-protein network of the identified endotype 1 related senescence genes with notable genes such as hub genes Sirtuin 1 (*SIRT1*), Mitogen-Activated Protein Kinase (*MAPK*)14, and cell proliferation regulators Forkhead Box O (*FOXO*)1 and Cyclin Dependent Kinase (*CDK*)2. Next, to understand which unique biological processes play a role this component we performed pathway analysis of the 24 genes marking senescence endotype 1 (Supplementary table 3). To identify unique senescence pathways, overlapping processes between endotype 1 and-2 were excluded. As shown in figure 2-B/C and supplementary table 5, significant pathway enrichment was found for the 24 genes marking senescence endotype 1, cell proliferating pathways such as "FOXO-mediated transcription of cell cycle genes" (R-HSA-9617828 FDR=4.4\*10<sup>-04</sup>) with involvement of *FOXI1/4* and RB Transcriptional Corepressor Like (*RBL*)2, "DNA Damage/Telomere Stress Induced Senescence" (R-HSA-2559586 FDR=1.4\*10<sup>-02</sup>) with involvement of *CDKN1B*, RB Transcriptional

Corepressor (*RB*)1 and *CDK*2 and signaling pathways such as "Intracellular signaling by second messengers" (R-HSA-9006925 FDR=1.5\*10<sup>-03</sup>) *RB*1 and *CDKN*1B. In other words and as exemplified (Figure 2A) and confirmed by RT-qPCR (Figure 3B), patients that are expressed in endotype 1 showed higher expression of these genes compared to patients that express endotype 2 (Figure 2A).

To gain further insight into possible treatments for endotype 1 patients, drug-gene interactions were investigated. When looking into previously known and approved drug-gene interactions, the 10 most significant differentially expressed genes of endotype 1, 70 drug-gene interactions were found (Supplementary table 7). Network analysis of this interaction showed a highly interconnected network, including many drug-drug interactions (Supplementary Figure 1). Worthy notions are metformin, rapamycin and dasatinib, which all showed direct connections to the top 10 genes. Metformin showed direct connections to TNF Receptor Superfamily Member (TNFRSF)11B, ATM Serine/Threonine Kinase (ATM), and SIRT1, rapamycin to MET Proto-Oncogene (MET), CDK2, RB1, ATM, and dasatinib to MET and MAPK14 (Supplementary Figure 1). This indicates the need for further analysis to select possible treatable targets.

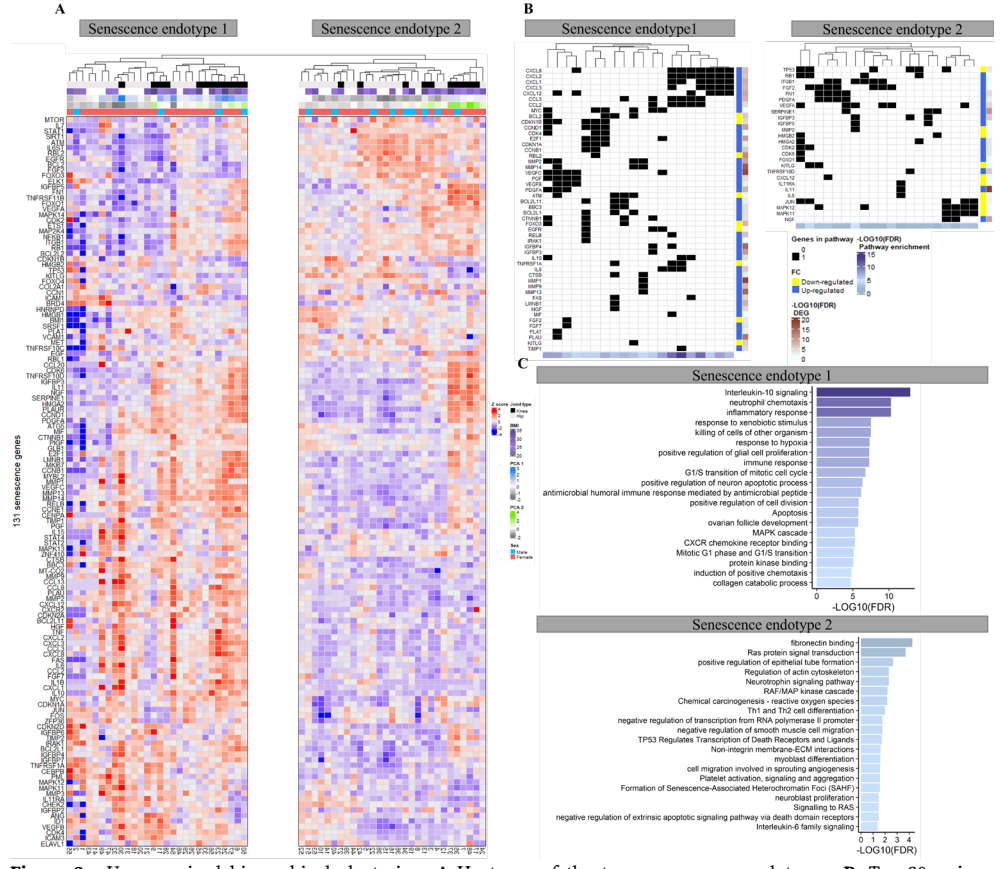


**Figure 2** - Unsupervised hierarchical clustering. **A** Heatmap of the two senescence endotypes. **B**, Top 20 unique significant enriched pathways of the two senescence endotypes with their respective genes in black. **C**, Barplot of the top 20 unique significant enriched pathways of the senescence endotypes. n=57

# Characteristics of senescence endotype 2 in aged articular cartilage

Figure 3A shows the protein-protein network of the identified endotype 2 related senescence genes with, among others notable SASP genes such as *MMP1/13*, Plasminogen Activator, Urokinase Receptor (*PLAUR*), chemokines; C-X-C Motif Chemokine Ligand (*CXCL*)1-3, *IL6* and *IGFBP4/6/7*. As shown in Figure 2B/C and supplementary table 6, pathway enrichment analysis of the 51 descriptive endotype 2 genes showed enrichment for inflammatory and signaling pathways, such as, "IL17 signaling pathway" (hsa04657 FDR=1.0\*10<sup>-13</sup>,Figure 2B/C) and "TNF signaling pathway" (hsa04668 FDR=2.8\*10<sup>-13</sup>, Figure 2B/C) represented by genes such as *IL6*, *CXCL1*-3 and *MMP3/9/14* and *VEGFC*, respectively. As well as inflammatory related diseases such as "Rheumatoid arthritis" (FDR=1.6\*10<sup>-09</sup>) with *MMP1/3* and *IL6*.

Analysis of drug-gene interactions of endotype 2 genes revealed 49 drug-gene interactions for the 10 most significantly differentially expressed genes in endotype 2 (supplementary table 8). Further network analysis showed for endotype 2 highly interconnected drug-gene and drug-drug interactions (Supplementary Figure 2). Notable drugs are doxycycline, zoledronic acid, alendronate and calcitriol, these drugs show a direct connection to the top 10 genes of endotype 2 and are located closely together in the network (Supplementary Figure 2). Doxycycline showed direct connection to *MMP2* and *MMP14*, zoledronic acid and alendronate to *MMP2* and calcitriol to *IGFBP4*, RELB Proto-Oncogene, NF-KB Subunit (*RELB*), *MMP14*, CXCL12 and *MMP2*. Where

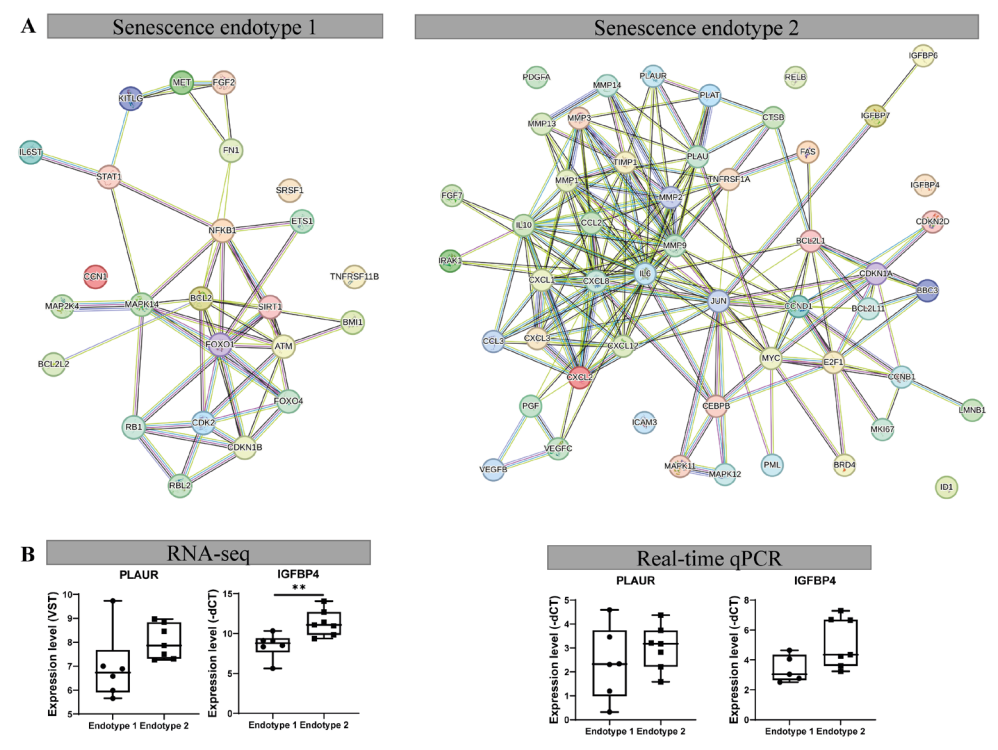


**Figure 3** - Characterization senescence endotypes. **A,** STRING protein-protein network of the endotypes using endotype describing genes. **B,** Technical validation of the genes expressed in the components. Measured by RNA-seq (left panel, n=13) and validated by real-time qPCR (right panel, n=8-13) showing senescence cartilage endotype 1 and -2. \*\*P<0.01, student t-test.

alendronate also showed direct connections to zoledronic acid and calcitriol.

Taken together, we could successfully stratify patients for 2 different senescent endotypes in human aged cartilage, endotype 1, marked by changes in cell proliferating pathways/absence of inflammation and increased expression of *FOXO1/4*, *RBL2* and *CDKN1B* and endotype 2, marked by inflammation/cell cycle regulating pathways and upregulated gene expression of *IL6*, *MMP1/3* and *VEGFC*. We have indicated possible drugs that target endotype-specific genes. These findings indicate different intrinsic expected survival pathways of patients. OA is closely related to age and is the result of age-related changes. This raises the question whether the senescence endotypes reflect a body wide senescence state rather than a tissue specific profile.

#### Metabolomic profiles in blood reflect a body wide senescence state

Since metabolic biomarkers are excellent aging biomarkers, we next set out to measure metabolic biomarkers using the 1H-NMR (Nightingale) platform and explored whether the tissue specific senescent endotypes identified in articular cartilage correspond to any profile in the circulation. Hereto, we measured metabolic biomarkers in 123 serum samples that had an overlap of 21 individuals for which we analyzed the RNA sequencing data of articular cartilage (The RAAK study). Metabolic biomarkers were excluded below a detection limit of 5 and PCA analysis was used to identify outliers (Supplementary Figure 3). To limit the chance of overfitting, 63 underived and independent metabolomic biomarkers were used for further analysis 17. These 63 metabolic biomarkers compose of lipids, fatty acids, amino acids and glycolysis-related metabolites. Unsupervised hierarchical clustering of the 63 independent metabolic biomarkers in the 21 overlapping patients resulted in two distinct metabolic clusters (Figure 1/ Figure 4A, Supplementary table 9) independent of BMI (FDR=4.2\*10-1, Supplementary table 10A). These two metabolic clusters corresponded for 81% to the articular cartilage endotypes, where metabolic endotype 1 corresponds to cartilage endotype 2 and metabolic endotype 2 with cartilage endotype 1 (Figure 2A/4A). Herein, the two endotypes appear to have opposite profiles with respect to lipids, apolipoproteins and fatty acids (Figure 4A and supplementary table 11). Senescence endotype 1 was marked by amino acids; Histidine (FDR=1.7\*10-2, Supplementary table 11) and Phenylalanine (FDR=2.3\*10-2). While senescence endotype 2 was marked by cholesterol (FDR=1.5\*10-20, Supplementary table 11), total lipids in low density lipids (with a diameter variating from 18.7nm-25.5nm, FDR=1.2\*10-27), apolipoproteins A1 and B (FDR=6.2\*10-4 FDR=3.0\*10-19, respectively) and fatty acids (FDR=9.86\*10-5) mainly by poly unsaturated fatty acids (PUFA, FDR=3.3\*10-5), Omega 3 and 6 (FDR=7.6\*10-6 and FDR=1.5\*10-4, respectively). Moreover, including all 123 patients with metabolic data confirmed that these metabolic clusters were robust (Figure 4B) independent of BMI (FDR=3.3\*10-1, Supplementary table 10B).

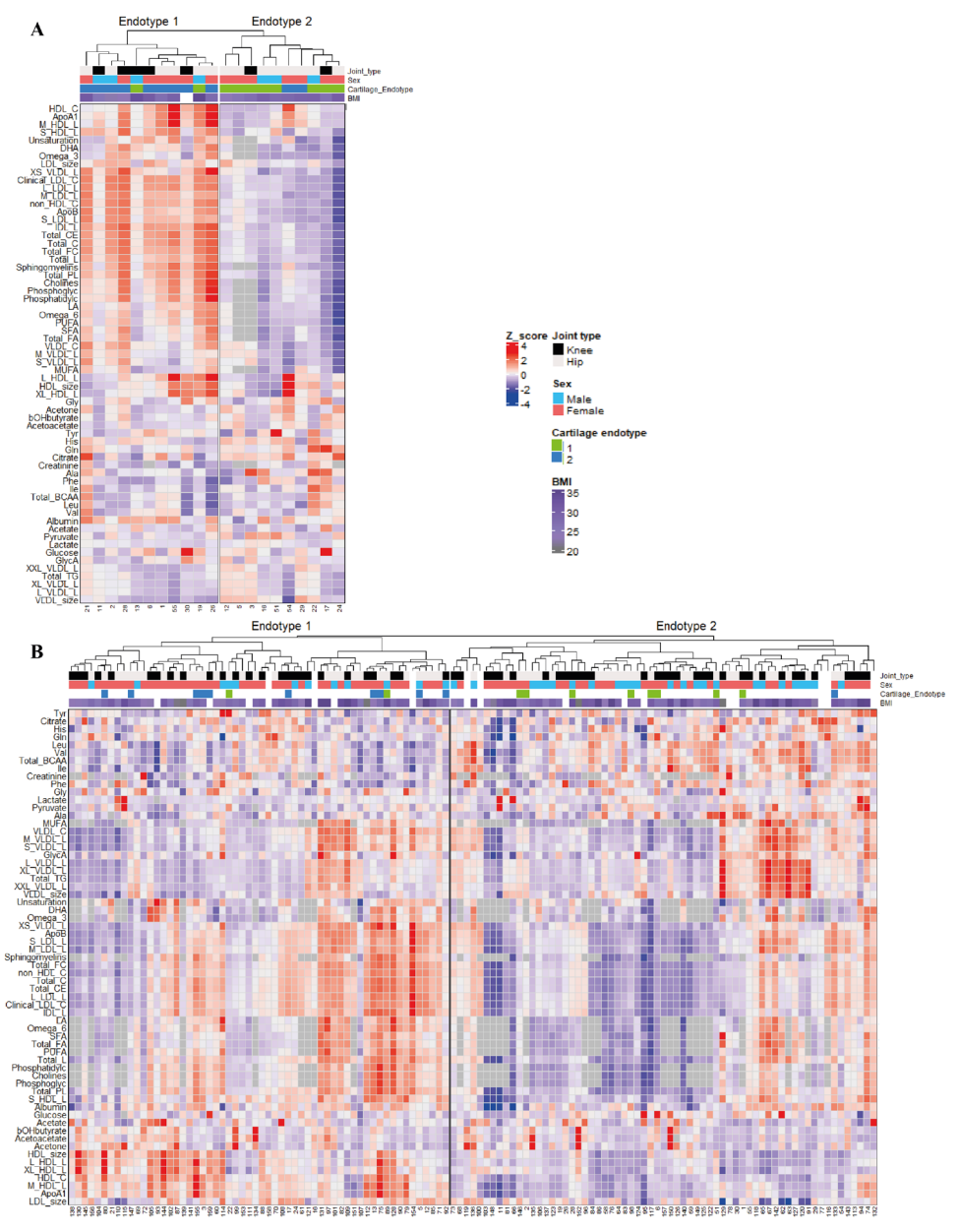


**Figure 4** - Serum metabolite measurements. Clustering of serum metabolite expression levels (Z-score) based on Spearman's correlation resulted in two similar clusters as on cartilage mRNA level **A**, in the overlapping dataset 81% was correctly clustered (n=21) **B**, in all metabolite samples, 86% was correctly clustered (n=123).

# Discussion

In the present study, senescent heterogeneity in aged articular cartilage was characterized and associated with circulating metabolic biomarkers. Based on the RNA sequencing profile of 131 expressed senescence genes, two robust cellular senescent endotypes were identified in aged articular cartilage. Notable was that unsupervised hierarchical clustering of 63 independent metabolic biomarkers resulted in two clusters that had a significant large overlap (81%) with the identified senescence endotypes in cartilage. Senescence endotype 1 was characterized in aged articular cartilage by genes involved in cell proliferation such as *FOXO4* and *CDKN1B* and concomitantly in plasma with amino acids such as histidine. Senescence endotype 2, on the other hand, was characterized by genes involved in SASP such as *IL6* and *MMP1/3* and alongside in serum with (low density) lipids, cholesterol and fatty acids. Finally, we explored drug-gene interactions of the endotype specific pathways that, together with the metabolic biomarkers, could facilitate patient-tailored targeting of senescence in OA.

The identified senescence endotype 1 in aged articular cartilage was characterized by FOXOmediated transcription of cell cycle genes and particularly FOXO4 and CDKN1B (encoding p27). These FOXO mediated proteins control several functions such as cell survival, growth and metabolism, likely reflecting the classic cell cycle arrest feature of senescence via p21 <sup>27,28</sup>. Herein, FOXO4 can directly bind to p53 when DNA damage occurs, activating p53-dependent transcription of p21 28. P27, part of the CDK inhibitor family is involved in the cell cycle progression and responsive to extracellular antiproliferative signals. Increased levels of p27 resulted in reduced levels of proliferation and cytoplasmic p27 regulates the actin skeleton, affecting cell migration <sup>29</sup>. The therapeutics identified for endotype 1 pathways, metformin, rapamycin and dasatinib, all affect FOXO-mediated transcription of cell cycle 30-33. Where metformin regulates FOXO proteins by regulating mechanistic Target Of Rapamycin Kinase (mTOR) signaling through 5'adenosine monophosphate-activated protein kinase (AMPK) activation, which in turn activates FOXO proteins <sup>30</sup> 31. Dasatinib inhibits phosphorylation of FOXO proteins, resulting in apoptosis and targets the phosphatidylinositol 3'-kinase- protein kinase B (PI3K-AKT) signaling pathway, which in its turn inhibits FOXO activity 32,33. This is in line with the increased blood metabolite levels of amino acids, able to regulate cell cycle arrest 34, of senescence endotype 1 patients. Taken together, the presence of important endotype 1 describing genes in FOXO mediated cell cycle regulation, (in)direct link of the drugs to the FOXO cell cycle regulation and increased levels of amino acids in the metabolic blood profile, suggest that endotype 1 patients could benefit from treatments targeting the FOXOmediated transcription of cell cycle pathway.

The identified senescence endotype 2 in aged articular cartilage was characterized inflammatory SASP pathways and particularly *IL6*, *MMP1/3*. IL6 is a main pro-inflammatory cytokine, MMP1 and 3 members of the MMP family and can control the factors present in the SASP by cleaving several soluble factors <sup>35</sup>. These MMPs are also present in the OA pathophysiology, cleaving main components of the cartilage matrix, collagen type 2 and aggrecan. The therapeutics identified for endotype 2 pathways, doxycycline, zoledronic acid, alendronate and calcitriol, all affect the inflammatory SASP <sup>36-39</sup>. Where doxycycline is a strong anti-inflammatory drug that can inhibit MMP activity as well as modulate cell proliferation and reduce the SASP release <sup>36,37</sup>. While zoledronic acid decreases the amount of senescent cells and dampens the SASP profile in-vitro in human lung fibroblasts as well as in-vivo in aged mice <sup>38</sup>. This is in line with the inflammatory metabolic

health of endotype 2 patients, marked by the increase of lipids, cholesterol and fatty acids <sup>40,41</sup>. The presence of important SASP genes, the anti-inflammatory effects of the drugs and presence of an inflammatory metabolic profile suggest that endotype 2 patients could benefit most from therapeutics targeting inflammatory SASP pathways and not only the cell cycle arrest pathways.

Prior to any clinical application, it should however be taken into account that the proposed pharmacological treatments are primarily put forward based on theoretical drug-gene interactions. Hence, comprehensive assessment, encompassing both the strength and weaknesses of the proposed pharmacological treatments is required as well as additional pre-clinical testing of drugs. We propose that such pre-clinical studies should preferably be done in aged human osteochondral explants challenged by hyper-physiological stress <sup>7</sup>.

The presence of two robust senescence endotypes in aged articular cartilage highlights heterogeneity in the response of chondrocytes upon environmental stressors throughout life. Particularly remarkable is that these cartilage specific endotypes were robustly reflected by two corresponding metabolomic profiles in the circulation, independent of BMI. Although these blood metabolic profiles could be directed entirely by the senescence endotype in articular cartilage, we feel that it is more likely the reflection of intrinsic, subject specific, survival strategy performed in all tissues. This particularly because chondrocytes are metabolically silent and reside in a non-perfused tissue 42. Moreover, Farr and colleagues 43 recently demonstrated that systemic administration of senolytics, hence body wide clearance, was more effective to reduce bone dysfunction as compared to local administration in mice. This support our notion that tissue specific senescent endotypes actually reflect intrinsic, subject specific, survival strategy performed in all tissues, whereas the metabolic profiles could facilitate patient-tailored treatment options for OA. In any case more studies are necessary to confirm these hypotheses, preferably by assessing senescence endotypes in other tissues that are subjected to age-related degenerative changes (e.g. muscle) and in comparison to metabolic profiles in the blood. Moreover, despite the fact that the two senescence endotypes were identified by unsupervised hierarchical clustering in two different molecular levels of information (transcriptomics and metabolomics), the robustness and generalizability of the two identified senescence endotypes needs to be further validated in independent cohorts. On a different note, if metabolic profiles indeed reflect intrinsic conditions in the body they could also originate from associated co-morbidities such as metabolic diseases or cardiovascular diseases. Consequently, the suggested pharmacological therapies may not be exclusive, hence requiring caution and pre-clinical testing prior to clinical applicability.

Taken together, our study showed two articular cartilage specific senescence endotypes with corresponding metabolic profiles in blood. Given that articular cartilage is a metabolically silent and non-perfused tissue, we advocate that the metabolic profiles in blood could be a reflection of an intrinsic, body wide, survival strategy of tissues. Consequently, these non-invasive metabolic profiles could function as biomarkers for patient-tailored targeting of senescence in OA and beyond.

# Acknowledgements

We thank all the participants of the RAAK study. The LUMC has and is supporting the RAAK study. We thank all the members of our group. We also thank Demiën Broekhuis, Enrike van der Linden, Robert van der Wal, Anika Rabelink-Hoogenstraaten, Peter van Schie, Shaho Hasan, Maartje Meijer, Daisy Latijnhouwers and Geert Spierenburg for collecting the RAAK material. We thank all participating patients and doctors at Alrijne Leiderdorp. We thank Rachid Mahdad for his contribution to the collection of joint tissue.

#### Sources of funding

The study was funded by VOILA – SMARTage (nr LSHM18093), the Dutch Arthritis Society (DAA\_10\_1-402) and the Dutch Scientific Research council NWO /ZonMW VICI scheme. Data is generated within the scope of the Medical Delta programs Regenerative Medicine 4D: Generating complex tissues with stem cells and printing technology and Improving Mobility with Technology.

#### Conflict of interest

PDK is founder, managing director and shareholder of Cleara Biotech B.V., a company developing compounds against cellular senescence.

# References

- Wu, Y., Goh, E. L., Wang, D. & Ma, S. Novel treatments for osteoarthritis: a recent update. Open Access Rheumatology: Research and Reviews Volume 10, 135-140 (2018). https://doi.org;10.2147/oarrr.s176666
- 2 Hodgkinson, T., Kelly, D. C., Curtin, C. M. & O'Brien, F. J. Mechanosignalling in cartilage: an emerging target for the treatment of osteoarthritis. *Nature Reviews Rheumatology* 18, 67-84 (2022). https://doi.org.10.1038/s41584-021-00724-w
- 3 López-Otín, C., Blasco, M. A., Partridge, L., Serrano, M. & Kroemer, G. The Hallmarks of Aging. Cell 153, 1194-1217 (2013). https://doi.org:10.1016/j.cell.2013.05.039
- 4 Coryell, P. R., Diekman, B. O. & Loeser, R. F. Mechanisms and therapeutic implications of cellular senescence in osteoarthritis. Nature Reviews Rheumatology 17, 47-57 (2021). https://doi.org;10.1038/s41584-020-00533-7
- 5 Jeon, O. H. et al. Local clearance of senescent cells attenuates the development of post-traumatic osteoarthritis and creates a pro-regenerative environment. Nat Med 23, 775-781 (2017). https://doi.org.10.1038/nm.4324
- 6 Jeon, O. H., David, N., Campisi, J. & Elisseeff, J. H. in Journal of Clinical Investigation Vol. 128 1229-1237 (American Society for Clinical Investigation, 2018).
- Houtman, E. et al. Elucidating mechano-pathology of osteoarthritis: transcriptome-wide differences in mechanically stressed aged human cartilage explants. Arthritis Research & Therapy 23 (2021). https://doi. org:10.1186/s13075-021-02595-8
- 8 Calcinotto, A. et al. Cellular senescence: Aging, cancer, and injury. Physiological Reviews 99, 1047-1078 (2019). https://doi.org;10.1152/physrev.00020.2018
- 9 McCulloch, K., Litherland, G. J. & Rai, T. S. in Aging Cell Vol. 16 210-218 (2017).
- Yuan, C. et al. Classification of four distinct osteoarthritis subtypes with a knee joint tissue transcriptome atlas. Bone Res 8, 38 (2020). https://doi.org;10.1038/s41413-020-00109-x
- Xu, M. et al. Transplanted Senescent Cells Induce an Osteoarthritis-Like Condition in Mice. The Journals of Gerontology Series A: Biological Sciences and Medical Sciences, glw154 (2016). https://doi.org:10.1093/gerona/glw154

- 12 Gasek, N. S., Kuchel, G. A., Kirkland, J. L. & Xu, M. Strategies for targeting senescent cells in human disease. Nature Aging 1, 870-879 (2021). https://doi.org;10.1038/s43587-021-00121-8
- Oo, W. M., Little, C., Duong, V. & Hunter, D. J. The Development of Disease-Modifying Therapies for Osteoarthritis (DMOADs): The Evidence to Date. *Drug Design, Development and Therapy* **Volume 15**, 2921-2945 (2021). https://doi.org:10.2147/dddt.s295224
- 14 Zhang, X. X. et al. Aging, Cell Senescence, the Pathogenesis and Targeted Therapies of Osteoarthritis. Front Pharmacol 12, 728100 (2021). https://doi.org.10.3389/fphar.2021.728100
- 15 Tripathi, U., Misra, A., Tchkonia, T. & Kirkland, J. L. Impact of Senescent Cell Subtypes on Tissue Dysfunction and Repair: Importance and Research Questions. *Mechanisms of Ageing and Development* 198, 111548 (2021). https://doi.org;10.1016/j.mad.2021.111548
- Van Den Akker, E. B. *et al.* Metabolic Age Based on the BBMRI-NL <sup>1</sup> H-NMR Metabolomics Repository as Biomarker of Age-related Disease. *Circulation: Genomic and Precision Medicine* 13, 541-547 (2020). https://doi.org:10.1161/circgen.119.002610
- Deelen, J. et al. A metabolic profile of all-cause mortality risk identified in an observational study of 44,168 individuals. Nature Communications 10 (2019). https://doi.org;10.1038/s41467-019-11311-9
- 18 Kuiper, L. M. et al. Evaluation of epigenetic and metabolomic biomarkers indicating biological age (Cold Spring Harbor Laboratory, 2022).
- 19 Coutinho De Almeida, R. et al. RNA sequencing data integration reveals an miRNA interactome of osteoarthritis cartilage. Annals of the Rheumatic Diseases 78, 270-277 (2019). https://doi.org.10.1136/annrheumdis-2018-213882
- 20 Gu, Z. Complex heatmap visualization. iMeta 1 (2022). https://doi.org:10.1002/imt2.43
- 21 Coutinho De Almeida, R. et al. Identification and characterization of two consistent osteoarthritis subtypes by transcriptome and clinical data integration. Rheumatology (2020). https://doi.org:10.1093/rheumatology/keaa391
- 22 Szklarczyk, D. et al. The STRING database in 2023: protein-protein association networks and functional enrichment analyses for any sequenced genome of interest. Nucleic Acids Res 51, D638-D646 (2023). https://doi.org:10.1093/nar/gkac1000
- 23 Sherman, B. T. et al. DAVID: a web server for functional enrichment analysis and functional annotation of gene lists (2021 update). Nucleic Acids Research 50, W216-W221 (2022). https://doi.org.10.1093/nar/gkac194
- 24 Freshour, S. L. et al. Integration of the Drug-Gene Interaction Database (DGIdb 4.0) with open crowdsource efforts. Nucleic Acids Research 49, D1144-D1151 (2021). https://doi.org;10.1093/nar/gkaa1084
- 25 Szklarczyk, D. et al. STITCH 5: augmenting protein-chemical interaction networks with tissue and affinity data. Nucleic Acids Res 44, D380-384 (2016). https://doi.org:10.1093/nar/gkv1277
- 26 Halekoh, U., Hojsgaard, S. & Yan, J. The R Package geepack for Generalized Estimating Equations. J Stat Softw 15, 1-11 (2006). https://doi.org;DOI 10.18637/jss.v015.i02
- 27 Bourgeois, B. & Madl, T. Regulation of cellular senescenceviathe FOXO4-p53 axis. FEBS Letters 592, 2083-2097 (2018). https://doi.org;10.1002/1873-3468.13057
- 28 Baar, M. P. et al. Targeted Apoptosis of Senescent Cells Restores Tissue Homeostasis in Response to Chemotoxicity and Aging. Cell 169, 132-147.e116 (2017). https://doi.org;10.1016/j.cell.2017.02.031
- 29 Pruitt, S. C., Freeland, A., Rusiniak, M. E., Kunnev, D. & Cady, G. K. Cdkn1b overexpression in adult mice alters the balance between genome and tissue ageing. *Nature Communications* 4 (2013). https://doi.org.10.1038/ncomms3626
- 30 Zou, G., Bai, J., Li, D. & Chen, Y. Effect of metformin on the proliferation, apoptosis, invasion and autophagy of ovarian cancer cells. Experimental and Therapeutic Medicine (2019). https://doi.org;10.3892/etm.2019.7803
- Queiroz, E. A. I. F. et al. Metformin Induces Apoptosis and Cell Cycle Arrest Mediated by Oxidative Stress, AMPK and FOXO3a in MCF-7 Breast Cancer Cells. PLoS ONE 9, e98207 (2014). https://doi.org;10.1371/journal. pone.0098207
- Pellicano, F. *et al.* The antiproliferative activity of kinase inhibitors in chronic myeloid leukemia cells is mediated by FOXO transcription factors. *Stem Cells* **32**, 2324-2337 (2014). https://doi.org:10.1002/stem.1748

- 33 Wang, L., Lankhorst, L. & Bernards, R. Exploiting senescence for the treatment of cancer. Nature Reviews Cancer 22, 340-355 (2022). https://doi.org;10.1038/s41568-022-00450-9
- 34 Saqcena, M. et al. Amino Acids and mTOR Mediate Distinct Metabolic Checkpoints in Mammalian G1 Cell Cycle. PLoS ONE 8, e74157 (2013), https://doi.org.10.1371/journal.pone.0074157
- 35 Coppé, J.-P., Desprez, P.-Y., Krtolica, A. & Campisi, J. The Senescence-Associated Secretory Phenotype: The Dark Side of Tumor Suppression. *Annual Review of Pathology: Mechanisms of Disease* 5, 99-118 (2010). https://doi. org:10.1146/annurev-pathol-121808-102144
- 36 Chang, W. Y., Clements, D. & Johnson, S. R. Effect of doxycycline on proliferation, MMP production, and adhesion in LAM-related cells. Am J Physiol Lung Cell Mol Physiol 299, L393-400 (2010). https://doi.org:10.1152/aiplung.00437.2009
- Li, X., Khan, D., Rana, M., Hänggi, D. & Muhammad, S. Doxycycline Attenuated Ethanol-Induced Inflammaging in Endothelial Cells: Implications in Alcohol-Mediated Vascular Diseases. *Antioxidants* 11, 2413 (2022). https://doi.org:10.3390/antiox11122413
- 38 Samakkarnthai, P. et al. In vitro and in vivo effects of zoledronic acid on senescence and senescence-associated secretory phenotype markers. Aging 15, 3331-3355 (2023). https://doi.org;10.18632/aging.204701
- 39 Zhu, S. et al. Alendronate protects against articular cartilage erosion by inhibiting subchondral bone loss in ovariectomized rats. Bone 53, 340-349 (2013). https://doi.org;10.1016/j.bone.2012.12.044
- 40 Andersen, C. J. Lipid Metabolism in Inflammation and Immune Function. Nutrients 14, 1414 (2022). https://doi. org:10.3390/nu14071414
- 41 Kotlyarov, S. & Kotlyarova, A. Involvement of Fatty Acids and Their Metabolites in the Development of Inflammation in Atherosclerosis. *International Journal of Molecular Sciences* 23, 1308 (2022). https://doi.org.10.3390/ ijms23031308
- 42 Zheng, L., Zhang, Z., Sheng, P. & Mobasheri, A. The role of metabolism in chondrocyte dysfunction and the progression of osteoarthritis. Ageing Res Rev 66, 101249 (2021). https://doi.org.10.1016/j.arr.2020.101249
- 43 Farr, J. N. et al. Local senolysis in aged mice only partially replicates the benefits of systemic senolysis. Journal of Clinical Investigation (2023). https://doi.org:10.1172/jci162519

# **Appendix A**

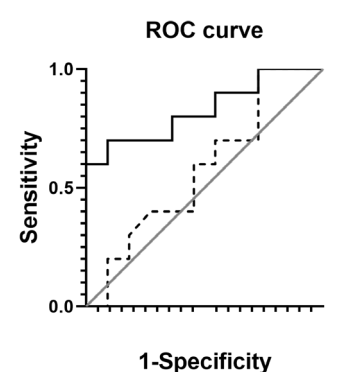
Besides the two overlapping molecular profiles on blood and cartilage level. We further explored the use of miRNAs as predictive non-invasive blood biomarkers. As seen in Table A1, using LASSO regression, we found a panel of 10 miRNAs delineating senescence endotype 2. Characterizing the correct predictions by these biomarkers showed that adding these miRNAs to baseline predictions using age sex and joint type improved the correct predictions from 58% to 83% (Figure A1). This suggest the potential of using miRNAs as diagnostic biomarkers. However, more interestingly would be to combine circulating miRNAs with blood-based metabolites and patient characteristics to increase the robustness of the prediction.

Table A1 - miRNAs of senescence endotype 2, selected by the LASSO regression.

hsa-miR-22-3p
hsa-miR-1307-3p
hsa-miR-195-3p
hsa-miR-4646-3p
hsa-miR-6503-3p
hsa-miR-195-5p
hsa-miR-1227-3p
hsa-miR-6873-3p
hsa-miR-6767-5p
hsa-miR-4742-3p
N=21

# Supplementary data

**Supplementary table 1** - Patients demographics of the 57 aged human articular cartilage samples as well as the endotypes present in aged human articular cartilage and GEE results between the two endotypes with formula: Endotype heatmap~Age+Sex\_BMI+joint type, Endotype heatmap~JSN + Osteophyte and Endotype heatmap ~ KL score.



**Figure A1** - Receiver operating curve (ROC) for circulating miRNAs for senescence endotype 2. Reflecting the area under the curve (AUC) of 58% for age sex and joint type (baseline, dashed line) and 83% for baseline with circulating miRNAs selected by the LASSO (black line), n=21.

	Preserved	cartilage	Endotype 1		Endotype	Endotype 2		stics		
		N		N		N	Beta	SE	P	N
Age (S.D.)	67.8(8.4)	56	49.8(7.8)	29	48.0(8.9)	27	0.08	0.05	0.16	39
Females	44	57	20	29	24	28	-1.20	0.72	0.10	39
Knee joints	35	57	10	29	12	28	-0.19	0.74	0.80	39
BMI (S.D.)	29.0(4.5)	39	24.1(4.0)	20	21.5(5.0)	19	0.10	0.10	0.32	39
JSN (S.D.)	4.4(1.5)	50	3.9 (1.5)	25	4.3 (1.4)	25	-0.17	0.19	0.33	50
Osteophyte	3.4(2.4)	50	3.8 (2.5)	25	3.0 (2.3)	25	0.14	0.13	0.27	50
KL score	2.7(0.6)	38	2.8 (0.7)	18	2.6 (0.5)	20	-0.79	0.52	0.13	38

**Supplementary table 2** - 155 senescence genes found in literature with their respective RNA-seq expression levels and quartile in preserved tissue (Mean Preserved, MP; Quartile Preserved, QP) and lesioned tissue (Mean Lesioned, ML; Quartile Lesioned, QL). Column Papers represents the source where the senescent genes was found.

Ensemblenumber	Gene name	MP	QP	ML	QL	Papers
ENSG00000115414	FN1	18,9	4	19,7	4	Coppé, Jean-Philippe, et al. 2010
ENSG00000139219	COL2A1	17,4	4	17,3	4	Ashraf et al. 2016
ENSG00000170345	FOS	12,6	4	12,2	4	Gorospe, Myriam, and Kotb Abdelmohsen. (2011)
ENSG00000035862	TIMP2	12,3	4	12,4	4	Coppé, Jean-Philippe, et al. 2010
ENSG00000102265	TIMP1	12,3	4	12,5	4	Coppé, Jean-Philippe, et al. 2010
ENSG00000198712	MT-CO2	12,2	4	12,1	4	Coppé, Jean-Philippe, et al. 2010
ENSG00000142871	CCN1	12,1	4	12	4	Jun, J. I., & Lau, L. F. (2010).
ENSG00000164733	CTSB	11,9	4	11,9	4	Coppé, Jean-Philippe, et al. 2010
ENSG00000115461	IGFBP5	11,8	4	11,8	4	Coppé, Jean-Philippe, et al. 2010,Sanada, Fumihiro, et al. (2018)
ENSG00000112715	VEGFA	10,9	4	11,1	4	McCulloch, K., Litherland, G. J., & Rai, T. S. (2017)
ENSG00000164761	TNFRSF11B	10,9	4	12,1	4	Coppé, Jean-Philippe, et al. 2010
ENSG00000149968	MMP3	10,8	4	9,9	4	Coppé, Jean-Philippe, et al. (2010), Calcinotto, Arianna, et al. (2019), de Keizer, Peter LJ. (2017), Jeon, Ok Hee, et al. (2018), Jeon, Ok Hee, et al. (2017), McCulloch, K., Litherland, G. J., & Rai, T. S. (2017)
ENSG00000134352	IL6ST	10,7	4	10,7	4	Coppé, Jean-Philippe, et al. 2010
ENSG00000168036	CTNNB1	10,7	4	10,9	4	de Keizer, Peter LJ. (2017)
ENSG00000087245	MMP2	10,5	4	9,8	4	Coppé, Jean-Philippe, et al. 2010
ENSG00000163453	IGFBP7	10,4	4	10,8	4	Coppé, Jean-Philippe, et al. 2010
ENSG00000157227	MMP14	10,4	4	10,5	4	Coppé, Jean-Philippe, et al. 2010
ENSG00000150093	ITGB1	10,3	4	10,5	4	Gorospe, Myriam, and Kotb Abdelmohsen. (2011)
ENSG00000138685	FGF2	10,2	4	10,4	4	Coppé, Jean-Philippe, et al. 2010
ENSG00000162692	VCAM1	10,2	4	9,9	4	Jeon, Ok Hee, et al. (2018)
ENSG00000141753	IGFBP4	10	4	10,5	4	Coppé, Jean-Philippe, et al. 2010
ENSG00000106366	SERPINE1	9,8	4	10,8	4	Coppé, Jean-Philippe, et al. 2010

Ensemblenumber	Gene name	MP	QP	ML	QL	Papers
ENSG00000067182	TNFRSF1A	9,8	4	9,7	4	Coppé, Jean-Philippe, et al. 2010
ENSG00000150907	FOXO1	9,8	4	9,9	4	Baar et al. 2017
ENSG00000128016	ZFP36	9,5	4	9,1	4	Gorospe, Myriam, and Kotb Abdelmohsen. (2011)
ENSG00000118689	FOXO3	9,4	4	9,2	4	Baar et al. 2017
ENSG00000177606	JUN	9,3	4	9,2	4	Gorospe, Myriam, and Kotb Abdelmohsen. (2011)
ENSG00000134954	ETS1	9,3	4	9,1	4	Gorospe, Myriam, and Kotb Abdelmohsen. (2011)
ENSG00000149311	ATM	9,3	4	9,2	4	Lopes-Paciencia, Stéphane, et al. (2019), Calcinotto, Arianna, et al. (2019)
ENSG00000167779	IGFBP6	9,3	4	9,7	4	Coppé, Jean-Philippe, et al. 2010
ENSG00000189403	HMGB1	9,2	4	9,5	4	Jeon, Ok Hee, et al. (2017)
ENSG00000125968	ID1	9,2	4	9,3	4	Gorospe, Myriam, and Kotb Abdelmohsen. (2011)
ENSG00000090339	ICAM1	9,1	4	8,6	4	Coppé, Jean-Philippe, et al. 2010
ENSG00000115415	STAT1	9,1	4	9,2	4	Baar et al. 2017, Ji, Juan, et al. (2017)
ENSG00000103479	RBL2	9,1	4	8,9	4	Baar 2017, Philipot et al. 2014
ENSG00000170581	STAT2	8,8	4	8,8	4	Baar et al. 2017, Ji, Juan, et al. (2017)
ENSG00000136450	SRSF1	8,7	4	8,9	4	Gorospe, Myriam, and Kotb Abdelmohsen. (2011)
ENSG00000172216	CEBPB	8,7	4	8,5	4	Calcinotto, Arianna, et al. (2019)
ENSG00000146674	IGFBP3	8,7	4	9,6	4	Coppé, Jean-Philippe, et al. 2010
ENSG00000110092	CCND1	8,6	4	9,1	4	Gorospe, Myriam, and Kotb Abdelmohsen. (2011)
ENSG00000141867	BRD4	8,6	4	8,3	4	Calcinotto, Arianna, et al. (2019)
ENSG00000138668	HNRNPD	8,6	4	8,6	4	Gorospe, Myriam, and Kotb Abdelmohsen. (2011)
ENSG00000124762	CDKN1A	8,5	4	8,7	4	Dai, Sheng-Ming, et al. (2006),Baar, Marjolein P., et al. (2017), Muñoz-Espín, Daniel, et al. (2013), de Keizer, Peter LJ. (2017)
ENSG00000171791	BCL2	8,5	4	8,7	4	Coryell, Philip R., Brian O. Diekman, and Richard F. Loeser. (2021)
ENSG00000146648	EGFR	8,4	4	8,2	4	Coppé, Jean-Philippe, et al. 2010
ENSG00000184216	IRAK1	8,4	4	8,6	4	Gorospe, Myriam, and Kotb Abdelmohsen. (2011)
ENSG00000198793	MTOR	8,3	4	8,4	4	Coryell, Philip R., Brian O. Diekman, and Richard F. Loeser. (2021), Calcinotto, Arianna, et al. (2019)
ENSG00000140464	PML	8,2	4	8	4	Rodier, Francis, et al. (2011)
ENSG00000173530	TNFRSF10D	8,2	4	8,5	4	Calcinotto, Arianna, et al. (2019)
ENSG00000135446	CDK4	8,2	4	8,3	4	Dai, Sheng-Ming, et al. (2006)
ENSG00000066044	ELAVL1	7,9	4	7,9	4	Gorospe, Myriam, and Kotb Abdelmohsen. (2011)
ENSG00000170266	GLB1	7,9	4	8,2	4	Muñoz-Espín, Daniel, et al. (2013), Krishnamurthy, Janakiraman, et al. (2004), Jeon, Ok Hee, et al. (2017)
ENSG00000173511	VEGFB	7,9	4	8	4	Coppé, Jean-Philippe, et al. 2010
ENSG00000111276	CDKN1B	7,8	4	7,7	4	Muñoz-Espín, Daniel, et al. (2013)

Ensemblenumber	Gene name	MP	QP	ML	QL	Papers
ENSG00000011422	PLAUR	7,7	4	8,5	4	Coppé, Jean-Philippe, et al. 2010
ENSG00000105810	CDK6	7,7	4	8,3	4	Dai, Sheng-Ming, et al. (2006)
ENSG00000112062	MAPK14	7,6	4	7,8	4	Dai, Sheng-Ming, et al. (2006). Jeon, Ok Hee, et al. (2018)
ENSG00000171552	BCL2L1	7,6	4	7,9	4	de Keizer, Peter LJ. (2017)
ENSG00000129473	BCL2L2	7,6	4	7,7	4	de Keizer, Peter LJ. (2017)
ENSG00000109320	NFKB1	7,6	4	7,7	4	Coryell, Philip R., Brian O. Diekman, and Richard F. Loeser. (2021), Jeon, Ok Hee, et al. (2018)
ENSG00000049130	KITLG	7,5	4	7,3	3	Coppé, Jean-Philippe, et al. 2010
ENSG00000197461	PDGFA	7,5	4	8	4	Demaria, Marco, et al. (2014)
ENSG00000164104	HMGB2	7,5	4	7,4	3	Calcinotto, Arianna, et al. (2019), Lopes-Paciencia, Stéphane, et al. (2019)
ENSG00000168283	BMI1	7,4	4	7,6	4	Gorospe, Myriam, and Kotb Abdelmohsen. (2011)
ENSG00000139687	RB1	7,3	3	7,3	3	Dai, Sheng-Ming, et al. (2006). Jeon, Ok Hee, et al. (2018)
ENSG00000137070	IL11RA	7,3	3	7	3	Coppé, Jean-Philippe, et al. 2010
ENSG00000141510	TP53	7,2	3	7	3	Muñoz-Espín, Daniel, et al. (2013),Krishnamurthy, Janakiraman, et al. (2004),Rodier, Francis, et al. (2011),Coppé, Jean-Philippe, et al. (2008), Dai, Sheng- Ming, et al. (2006), Jeon, Ok Hee, et al. (2017).
ENSG00000136997	MYC	7,1	3	7,2	3	Gorospe, Myriam, and Kotb Abdelmohsen. (2011)
ENSG00000126767	ELK1	7,1	3	6,9	3	Gorospe, Myriam, and Kotb Abdelmohsen. (2011)
ENSG00000137745	MMP13	7,1	3	6,7	3	Coppé, Jean-Philippe, et al. 2010
ENSG00000065559	MAP2K4	7	3	7,1	3	Gorospe, Myriam, and Kotb Abdelmohsen. (2011)
ENSG00000123374	CDK2	7	3	7	3	Gorospe, Myriam, and Kotb Abdelmohsen. (2011)
ENSG00000096717	SIRT1	6,9	3	6,8	3	Gorospe, Myriam, and Kotb Abdelmohsen. (2011)
ENSG00000105976	MET	6,9	3	7,3	3	Gorospe, Myriam, and Kotb Abdelmohsen. (2011)
ENSG00000100985	MMP9	6,9	3	6,4	3	Coppé, Jean-Philippe, et al. 2010
ENSG00000115457	IGFBP2	6,7	3	6,4	3	Coppé, Jean-Philippe, et al. 2010
ENSG00000119630	PGF	6,5	3	6,7	3	Coppé, Jean-Philippe, et al. 2010
ENSG00000129355	CDKN2D	6,5	3	6,7	3	Muñoz-Espín, Daniel, et al. (2013)
ENSG00000107562	CXCL12	6,4	3	6	3	Coppé, Jean-Philippe, et al. 2010
ENSG00000151665	PIGF	6,4	3	6,6	3	Coppé, Jean-Philippe, et al. 2010
ENSG00000184481	FOXO4	6,3	3	6,4	3	Baar et al. 2017
ENSG00000057663	ATG5	6,2	3	6,4	3	McCulloch, K., Litherland, G. J., & Rai, T. S. (2017)
ENSG00000240972	MIF	6,1	3	6,6	3	Coppé, Jean-Philippe, et al. 2010
ENSG00000095752	IL11	6,1	3	8,7	4	Coppé, Jean-Philippe, et al. 2010
ENSG00000076662	ICAM3	6	3	6,2	3	Coppé, Jean-Philippe, et al. 2010

Ensemblenumber	Gene name	MP	QP	ML	QL	Papers
ENSG00000214274	ANG	5,9	3	6,1	3	Coppé, Jean-Philippe, et al. 2010
ENSG00000188130	MAPK12	5,9	3	5,7	2	Dai, Sheng-Ming, et al. (2006). Jeon, Ok Hee, et al. (2018)
ENSG00000183765	CHEK2	5,9	3	6	3	Coppé, Jean-Philippe, et al. 2010
ENSG00000104368	PLAT	5,9	3	6,3	3	Coppé, Jean-Philippe, et al. 2010
ENSG00000122861	PLAU	5,8	2	5,5	2	Coppé, Jean-Philippe, et al. 2010
ENSG00000104856	RELB	5,6	2	5,8	3	Coryell, Philip R., Brian O. Diekman, and Richard F. Loeser. (2021)
ENSG00000156711	MAPK13	5,6	2	5,6	2	Dai, Sheng-Ming, et al. (2006). Jeon, Ok Hee, et al. (2018)
ENSG00000185386	MAPK11	5,6	2	5,3	2	Dai, Sheng-Ming, et al. (2006). Jeon, Ok Hee, et al. (2018)
ENSG00000153094	BCL2L11	5,4	2	5,4	2	Baar et al. 2017
ENSG00000108691	CCL2	5,4	2	5,1	2	de Keizer, Peter LJ. (2017)
ENSG00000134259	NGF	5,4	2	6,9	3	Coppé, Jean-Philippe, et al. 2010
ENSG00000080839	RBL1	5,4	2	5,6	2	Baar 2017, Philipot et al. 2014
ENSG00000140285	FGF7	5,4	2	5,3	2	Coppé, Jean-Philippe, et al. 2010
ENSG00000026103	FAS	5,2	2	5,2	2	Coppé, Jean-Philippe, et al. 2010
ENSG00000148773	MKI67	5	2	5,7	2	Calcinotto, Arianna, et al. (2019)
ENSG00000150630	VEGFC	5	2	5,2	2	Coppé, Jean-Philippe, et al. 2010
ENSG00000105327	BBC3	4,7	2	4,9	2	Baar et al. 2017
ENSG00000134057	CCNB1	4,6	2	5	2	Gorospe, Myriam, and Kotb Abdelmohsen. (2011)
ENSG00000169429	CXCL8	4,6	2	4,6	2	Coppé, Jean-Philippe, et al. 2010, de Keizer, Peter LJ. (2017), Philipot et al. (2014)
ENSG00000149948	HMGA2	4,5	2	5,2	2	Gorospe, Myriam, and Kotb Abdelmohsen. (2011)
ENSG00000196611	MMP1	4,4	2	4,4	2	Coppé, Jean-Philippe, et al. 2010, Calcinotto, Arianna, et al. (2019)
ENSG00000113368	LMNB1	4,4	2	4,7	2	Demaria, Marco, et al. (2014)
ENSG00000101412	E2F1	4,4	2	4,8	2	Dai, Sheng-Ming, et al. (2006)
ENSG00000277632	CCL3	4,3	2	4,3	2	Coppé, Jean-Philippe, et al. 2010
ENSG00000173535	TNFRSF10C	4,3	2	4,4	2	Coppé, Jean-Philippe, et al. 2010
ENSG00000119725	ZNF410	4,1	1	4,2	2	Philipot et al. 2014
ENSG00000136634	IL10	3,9	1	3,7	1	Jeon, Ok Hee, et al. (2018)
ENSG00000104432	IL7	3,9	1	3,7	1	Coryell, Philip R., Brian O. Diekman, and Richard F. Loeser. (2021)
ENSG00000147889	CDKN2A	3,9	1	4	1	Jeon, Ok Hee, et al. (2018), Demaria, Marco, et al. (2014), Baar 2017, Philipot et al. 2014, Jeon, Ok Hee, et al. (2017)
ENSG0000138378	STAT4	3,8	1	3,8	1	Baar et al. 2017, Ji, Juan, et al. (2017)

Ensemblenumber	Gene name	MP	QP	ML	QL	Papers
ENSG00000105173	CCNE1	3,8	1	4,1	1	Gorospe, Myriam, and Kotb Abdelmohsen. (2011)
ENSG00000081041	CXCL2	3,7	1	3,6	1	Coppé, Jean-Philippe, et al. 2010
ENSG00000136244	IL6	3,6	1	3,4	1	Coppé, Jean-Philippe, et al. 2010, Jeon, Ok Hee, et al. (2017), de Keizer, Peter LJ. (2017)
ENSG00000019991	HGF	3,6	1	3,3	1	Coppé, Jean-Philippe, et al. 2010
ENSG00000115009	CCL20	3,6	1	4	1	Coppé, Jean-Philippe, et al. 2010
ENSG00000164136	IL15	3,6	1	3,6	1	Coppé, Jean-Philippe, et al. 2010
ENSG00000101057	MYBL2	3,6	1	4,1	1	Gorospe, Myriam, and Kotb Abdelmohsen. (2011)
ENSG00000138798	EGF	3,6	1	3,8	1	Coppé, Jean-Philippe, et al. 2010
ENSG00000232810	TNF	3,6	1	3,5	1	Jeon, Ok Hee, et al. (2018)
ENSG00000180871	CXCR2	3,5	1	3,6	1	Coppé, Jean-Philippe, et al. 2010
ENSG00000163734	CXCL3	3,4	1	3,4	1	Coppé, Jean-Philippe, et al. 2010
ENSG00000163739	CXCL1	3,4	1	3,3	1	Coppé, Jean-Philippe, et al. 2010
ENSG00000108700	CCL8	3,4	1	3,2	1	Coppé, Jean-Philippe, et al. 2010
ENSG00000125538	IL1B	3,3	1	3,3	1	Coppé, Jean-Philippe, et al. 2010
ENSG00000115163	CENPA	3,3	1	3,6	1	Jeon, Ok Hee, et al. (2017), Coppé, Jean-Philippe, et al. 2010
ENSG00000181374	CCL13	3,2	1	3,2	1	Coppé, Jean-Philippe, et al. 2010
ENSG00000173077	DEC1	NA	NA	NA	NA	Calcinotto, Arianna, et al. (2019)
ENSG00000136574	GATA4	NA	NA	NA	NA	Calcinotto, Arianna, et al. (2019)
ENSG00000157168	NRG1	NA	NA	NA	NA	Coppé, Jean-Philippe, et al. 2010
ENSG00000124882	EREG	NA	NA	NA	NA	Coppé, Jean-Philippe, et al. 2010
ENSG00000137673	MMP7	NA	NA	NA	NA	Coppé, Jean-Philippe, et al. 2010
ENSG00000169194	IL13	NA	NA	NA	NA	Coppé, Jean-Philippe, et al. 2010
ENSG00000166670	MMP10	NA	NA	NA	NA	Coppé, Jean-Philippe, et al. 2010
ENSG00000163735	CXCL5	NA	NA	NA	NA	Coppé, Jean-Philippe, et al. 2010
ENSG00000109321	AREG	NA	NA	NA	NA	Coppé, Jean-Philippe, et al. 2010
ENSG00000006606	CCL26	NA	NA	NA	NA	Coppé, Jean-Philippe, et al. 2010
ENSG00000124875	CXCL6	NA	NA	NA	NA	Coppé, Jean-Philippe, et al. 2010
ENSG00000262406	MMP12	NA	NA	NA	NA	Coppé, Jean-Philippe, et al. 2010
ENSG00000108688	CCL7	NA	NA	NA	NA	Coppé, Jean-Philippe, et al. 2010
ENSG00000108342	CSF3	NA	NA	NA	NA	Coppé, Jean-Philippe, et al. 2010
ENSG00000275152	CCL16	NA	NA	NA	NA	Coppé, Jean-Philippe, et al. 2010
ENSG00000197632	SERPINB2	NA	NA	NA	NA	Coppé, Jean-Philippe, et al. 2010
ENSG00000164400	CSF2	NA	NA	NA	NA	Coppé, Jean-Philippe, et al. 2010
ENSG00000115008	IL1A	NA	NA	NA	NA	Coppé, Jean-Philippe, et al. 2010
ENSG00000113525	IL5	NA	NA	NA	NA	Coppé, Jean-Philippe, et al. 2010
ENSG00000172156	CCL11	NA	NA	NA	NA	de Keizer, Peter LJ. (2017)

Ensemblenumber	Gene name	MP	QP	ML	QL	Papers
ENSG00000133101	CCNA1	NA	NA	NA	NA	Gorospe, Myriam, and Kotb Abdelmohsen. (2011)
ENSG00000213927	CCL27	NA	NA	NA	NA	Jeon, Ok Hee, et al. (2018)
ENSG00000111537	IFNG	NA	NA	NA	NA	Jeon, Ok Hee, et al. (2018)
ENSG00000197919	IFNA1	NA	NA	NA	NA	Ji, Juan, et al. (2017)

QP= Quartile of expression in preserved cartilage (20048 genes in total). Standard deviation of preserved cartilage genes=2.0, min=2.7 counts, max=18.9 counts, QL= Quartile of expression in lesioned cartilage (20048 genes in total). Standard deviation of preserved cartilage genes=2.0, min=2.8 counts, max=19.7 counts

Supplementary table 3 - The 24 differentially expressed senescence genes for endotype 1

ensembl_gene_id	external_gene_name	FC <sup>1</sup>	FDR
ENSG00000103479	RBL2	-0,98	1,17E-15
ENSG00000138685	FGF2	-1,18	1,96E-11
ENSG00000096717	SIRT1	-0,81	9,11E-09
ENSG00000134352	IL6ST	-0,75	1,00E-07
ENSG00000171791	BCL2	-1,12	1,34E-06
ENSG00000049130	KITLG	-1,36	2,70E-06
ENSG00000134954	ETS1	-0,58	4,35E-05
ENSG00000164761	TNFRSF11B	-1,23	7,43E-05
ENSG00000065559	MAP2K4	-0,38	7,59E-05
ENSG00000139687	RB1	-0,45	1,35E-04
ENSG00000129473	BCL2L2	-0,39	2,02E-04
ENSG00000112062	MAPK14	-0,27	3,40E-04
ENSG00000115415	STAT1	-0,49	8,12E-04
ENSG00000149311	ATM	-0,66	1,57E-03
ENSG00000123374	CDK2	-0,28	3,57E-03
ENSG00000184481	FOXO4	-0,34	4,21E-03
ENSG00000168283	BMI1	-0,58	4,43E-03
ENSG00000105976	MET	-0,52	5,67E-03
ENSG00000136450	SRSF1	-0,27	1,11E-02
ENSG00000109320	NFKB1	-0,24	1,77E-02
ENSG00000111276	CDKN1B	-0,37	2,31E-02
ENSG00000115414	FN1	-0,62	2,31E-02
ENSG00000150907	FOXO1	-0,41	2,49E-02
ENSG00000142871	CCN1	-0,46	3,48E-02

<sup>&</sup>lt;sup>1</sup>FC = Fold change with endotype 1 as baseline. <sup>2</sup>FDR=False discovery rate, n=57.

 $\textbf{Supplementary table 4-} \ \text{The 51 differentially expressed senescence genes for endotype 2}$ 

ensembl_gene_id	Gene name	FC <sup>1</sup>	FDR <sup>2</sup>	ensembl_gene_id	Gene name	FC¹	FDR <sup>2</sup>
ENSG00000196611	MMP1	5,64	1,05E-18	ENSG00000140464	PML	0,65	3,40E-04
ENSG00000107562	CXCL12	3,78	9,51E-15	ENSG00000026103	FAS	0,85	5,94E-04
ENSG00000122861	PLAU	3	7,41E-14	ENSG00000110092	CCND1	0,73	8,07E-04
ENSG00000087245	MMP2	2,51	1,76E-13	ENSG00000153094	BCL2L11	0,65	8,07E-04
ENSG00000157227	MMP14	1,53	7,23E-12	ENSG00000113368	LMNB1	1,03	8,12E-04
ENSG00000141753	IGFBP4	2,34	1,04E-10	ENSG00000148773	MKI67	1,62	9,50E-04
ENSG00000277632	CCL3	3,8	1,36E-10	ENSG00000134057	CCNB1	0,72	1,02E-03
ENSG00000163739	CXCL1	4,5	7,53E-10	ENSG00000067182	TNFRSF1A	0,27	1,72E-03
ENSG00000104856	RELB	1,19	2,11E-09	ENSG00000177606	JUN	0,94	1,98E-03
ENSG00000163734	CXCL3	3,76	7,60E-09	ENSG00000149968	MMP3	1,06	2,01E-03
ENSG00000081041	CXCL2	3,5	9,11E-09	ENSG00000102265	TIMP1	0,82	2,50E-03
ENSG00000137745	MMP13	2,98	1,63E-08	ENSG00000076662	ICAM3	0,53	2,88E-03
ENSG00000136634	IL10	1,69	2,18E-08	ENSG00000101412	E2F1	0,96	2,88E-03
ENSG00000105327	BBC3	1,08	2,18E-08	ENSG00000125968	ID1	0,62	4,03E-03
ENSG00000173511	VEGFB	0,94	1,19E-07	ENSG00000167779	IGFBP6	0,79	4,43E-03
ENSG00000169429	CXCL8	2,86	1,55E-07	ENSG00000197461	PDGFA	0,5	4,64E-03
ENSG00000136244	IL6	3,25	2,84E-07	ENSG00000119630	PGF	0,88	5,97E-03
ENSG00000150630	VEGFC	1,71	5,67E-07	ENSG00000136997	MYC	0,55	1,24E-02
ENSG00000184216	IRAK1	0,51	6,69E-07	ENSG00000124762	CDKN1A	0,56	1,33E-02
ENSG00000100985	MMP9	3,28	1,20E-06	ENSG00000011422	PLAUR	0,71	2,12E-02
ENSG00000108691	CCL2	1,89	1,38E-06	ENSG00000129355	CDKN2D	0,44	2,43E-02
ENSG00000172216	CEBPB	1,06	1,17E-05	ENSG00000104368	PLAT	0,62	2,43E-02
ENSG00000171552	BCL2L1	0,38	2,48E-05	ENSG00000141867	BRD4	0,48	2,77E-02
ENSG00000163453	IGFBP7	0,77	4,17E-05	ENSG00000140285	FGF7	0,88	3,37E-02
ENSG00000164733	CTSB	0,52	1,34E-04	ENSG00000188130	MAPK12	0,5	4,72E-02

<sup>&</sup>lt;sup>1</sup>FC = Fold change with endotype 1 as baseline. <sup>2</sup>FDR=False discovery rate, n=57.

**Supplementary table 5** - significant(FDR<0.05) and unique pathways of endotype 1 using DAVID.

	71 0
Term	FDR
GO:1990841~promoter-specific chromatin binding	4,07E-06
hsa05165:Human papillomavirus infection	4,15E-05
GO:0045944~positive regulation of transcription from RNA polymerase II promoter	1,06E-04
R-HSA-2219528~PI3K/AKT Signaling in Cancer	2,07E-04
R-HSA-73857~RNA Polymerase II Transcription	2,07E-04
R-HSA-74160~Gene expression (Transcription)	3,73E-04
R-HSA-9617828~FOXO-mediated transcription of cell cycle genes	4,38E-04
R-HSA-9614085~FOXO-mediated transcription	5,31E-04
GO:0019899~enzyme binding	6,17E-04
GO:0090398~cellular senescence	6,17E-04
R-HSA-1643685~Disease	7,56E-04
R-HSA-1257604~PIP3 activates AKT signaling	8,59E-04
R-HSA-5663202~Diseases of signal transduction by growth factor receptors and second	1,34E-03
messengers	1,341-03
R-HSA-9006925~Intracellular signaling by second messengers	1,49E-03
hsa05203:Viral carcinogenesis	2,22E-03
R-HSA-9617629~Regulation of FOXO transcriptional activity by acetylation	6,39E-03
GO:0000785~chromatin	1,38E-02
R-HSA-2559586~DNA Damage/Telomere Stress Induced Senescence	1,42E-02
GO:0005654~nucleoplasm	1,81E-02
GO:0005634~nucleus	1,81E-02
R-HSA-69202~Cyclin E associated events during G1/S transition	1,98E-02
R-HSA-69656~Cyclin A:Cdk2-associated events at S phase entry	2,05E-02
GO:0006366~transcription from RNA polymerase II promoter	2,40E-02
GO:0042981~regulation of apoptotic process	2,40E-02
$hs a 0 4550 : Signaling\ pathways\ regulating\ pluripotency\ of\ stem\ cells$	2,43E-02
GO:0051721~protein phosphatase 2A binding	2,58E-02
GO:0007265~Ras protein signal transduction	2,81E-02
R-HSA-5674400~Constitutive Signaling by AKT1 E17K in Cancer	2,93E-02
GO:0097718~disordered domain specific binding	2,93E-02
GO:0060090~binding, bridging	2,93E-02
GO:0010629~negative regulation of gene expression	3,46E-02
GO:0051726~regulation of cell cycle	3,87E-02
hsa04917:Prolactin signaling pathway	4,75E-02
GO:0030308~negative regulation of cell growth	4,86E-02
R-HSA-5684996~MAPK1/MAPK3 signaling	4,87E-02
FDR = False discovery rate	

Supplementary table 6 - Drug-gene interactions for the 10 most significantly differentially expressed drugs of endotype 1

Gene	Drug	Gene	Drug
RBL2	SIROLIMUS	BCL2	ISOTRETINOIN
FGF2	VINCRISTINE	BCL2	PACLITAXEL
FGF2	FLUVOXAMINE	BCL2	VENETOCLAX
FGF2	LENALIDOMIDE	BCL2	TAZAROTENE
FGF2	INDOMETHACIN	BCL2	ETOPOSIDE
FGF2	PHENYLEPHRINE	BCL2	MITOXANTRONE
FGF2	SIROLIMUS	BCL2	FLOXURIDINE
FGF2	THALIDOMIDE	BCL2	DOXORUBICIN
FGF2	THYROTROPIN	BCL2	METHYLPREDNISOLONE
FGF2	TRIAMCINOLONE	BCL2	DOCETAXEL
FGF2	CAFFEINE	TNFRSF11B	EPINEPHRINE
FGF2	SUCRALFATE	TNFRSF11B	TESTOSTERONE
FGF2	ATORVASTATIN	TNFRSF11B	RISEDRONIC ACID
FGF2	FAMOTIDINE	TNFRSF11B	ANASTROZOLE
FGF2	ASPIRIN	TNFRSF11B	LETROZOLE
SIRT1	NIACINAMIDE	MAP2K4	COBIMETINIB
IL6ST	BAZEDOXIFENE	MAP2K4	TRAMETINIB
IL6ST	RALOXIFENE	MAP2K4	BINIMETINIB
BCL2	ERYTHROMYCIN	MAP2K4	ALCOHOL
BCL2	VINCRISTINE	RB1	EVEROLIMUS
BCL2	CARBOPLATIN	RB1	PALBOCICLIB
BCL2	ISOSORBIDE	RB1	TRAMETINIB
BCL2	EPIRUBICIN	RB1	PREDNISOLONE
BCL2	TRETINOIN	RB1	METHOTREXATE
BCL2	CISPLATIN	RB1	ALPELISIB
BCL2	BORTEZOMIB	RB1	BORTEZOMIB
BCL2	EDARAVONE	RB1	SIROLIMUS
BCL2	TENIPOSIDE	RB1	MERCAPTOPURINE
BCL2	PENTOXIFYLLINE	RB1	ASPARAGINASE
BCL2	RIBAVIRIN	RB1	LORLATINIB
BCL2	STREPTOZOCIN	RB1	FOSTAMATINIB
BCL2	OXALIPLATIN	RB1	RIBOCICLIB
BCL2	PHENYLBUTANOIC ACID	RB1	DEXAMETHASONE
BCL2	HYDROQUINONE	RB1	VORINOSTAT
BCL2	RALTITREXED	RB1	TOPOTECAN

**Supplementary table 7** - significant(FDR<0.05) and unique pathways of endotype 2 using DAVID.

Term	FDR
hsa04657:IL-17 signaling pathway	1,03E-13
GO:0005615~extracellular space	1,05E-13
hsa04668:TNF signaling pathway	2,84E-13
hsa05417:Lipid and atherosclerosis	1,44E-12
R-HSA-6783783~Interleukin-10 signaling	8,64E-10
hsa05323:Rheumatoid arthritis	1,59E-09
hsa04061:Viral protein interaction with cytokine and cytokine receptor	2,03E-09
hsa05142:Chagas disease	4,73E-09
GO:0008083~growth factor activity	1,80E-08
GO:0008009~chemokine activity	1,80E-08
hsa05163:Human cytomegalovirus infection	7,06E-08
hsa05219:Bladder cancer	7,42E-08
hsa04064:NF-kappa B signaling pathway	1,16E-07
R-HSA-1592389~Activation of Matrix Metalloproteinases	1,61E-07
R-HSA-168256~Immune System	2,63E-07
R-HSA-380108~Chemokine receptors bind chemokines	7,10E-07
GO:0030574~collagen catabolic process	8,06E-07
GO:0001666~response to hypoxia	8,06E-07
GO:0070098~chemokine-mediated signaling pathway	9,96E-07
GO:0045236~CXCR chemokine receptor binding	1,32E-06
GO:0004252~serine-type endopeptidase activity	1,73E-06
hsa04060:Cytokine-cytokine receptor interaction	1,79E-06
hsa04926:Relaxin signaling pathway	3,82E-06
GO:0006935~chemotaxis	3,90E-06
GO:0071222~cellular response to lipopolysaccharide	3,90E-06
GO:0048146~positive regulation of fibroblast proliferation	3,90E-06
GO:0071492~cellular response to UV-A	4,21E-06
GO:0071347~cellular response to interleukin-1	7,29E-06
GO:0022617~extracellular matrix disassembly	9,95E-06
GO:0050930~induction of positive chemotaxis	9,95E-06
GO:0001938~positive regulation of endothelial cell proliferation	1,03E-05
GO:0006954~inflammatory response	1,03E-05
R-HSA-1442490~Collagen degradation	1,80E-05
hsa05205:Proteoglycans in cancer	1,98E-05
GO:0001934~positive regulation of protein phosphorylation	2,15E-05
hsa05133:Pertussis	2,61E-05

Term	FDR
hsa05171:Coronavirus disease - COVID-19	2,61E-05
GO:0042056~chemoattractant activity	2,67E-05
GO:0004175~endopeptidase activity	6,46E-05
hsa04210:Apoptosis	7,61E-05
GO:0030593~neutrophil chemotaxis	9,06E-05
R-HSA-1474228~Degradation of the extracellular matrix	1,02E-04
R-HSA-375276~Peptide ligand-binding receptors	1,81E-04
hsa04932:Non-alcoholic fatty liver disease	1,81E-04
GO:0043524~negative regulation of neuron apoptotic process	2,14E-04
GO:0050918~positive chemotaxis	2,14E-04
GO:0097421~liver regeneration	2,30E-04
GO:0008285~negative regulation of cell proliferation	2,30E-04
GO:0031640~killing of cells of other organism	2,69E-04
GO:1904645~response to beta-amyloid	3,06E-04
GO:0009410~response to xenobiotic stimulus	3,06E-04
GO:0006508~proteolysis	3,06E-04
GO:0001541~ovarian follicle development	3,20E-04
GO:0051781~positive regulation of cell division	3,44E-04
hsa04630:JAK-STAT signaling pathway	3,49E-04
hsa04115:p53 signaling pathway	3,49E-04
R-HSA-1474244~Extracellular matrix organization	3,51E-04
$R-HSA-381426-Regulation of Insulin-like Growth Factor (IGF) transport\\$ and uptake by Insulin-like Growth Factor Binding Proteins (IGFBPs)	3,82E-04
R-HSA-2559582~Senescence-Associated Secretory Phenotype (SASP)	3,82E-04
GO:0004222~metalloendopeptidase activity	4,18E-04
hsa05130:Pathogenic Escherichia coli infection	4,94E-04
hsa05170:Human immunodeficiency virus 1 infection	4,99E-04
hsa05146:Amoebiasis	6,29E-04
hsa04015:Rap1 signaling pathway	6,73E-04
hsa05210:Colorectal cancer	6,73E-04
GO:0060252~positive regulation of glial cell proliferation	9,44E-04
hsa04625:C-type lectin receptor signaling pathway	9,59E-04
GO:0005102~receptor binding	1,08E-03
R-HSA-9006934~Signaling by Receptor Tyrosine Kinases	1,09E-03
hsa05134:Legionellosis	1,14E-03
hsa04062:Chemokine signaling pathway	1,22E-03
GO:0006955~immune response	1,30E-03

Term	FDR
GO:0061844~antimicrobial humoral immune response mediated by antimicrobial peptide	1,41E-03
GO:0005172~vascular endothelial growth factor receptor binding	1,74E-03
GO:0010628~positive regulation of gene expression	1,87E-03
GO:0043065~positive regulation of apoptotic process	1,93E-03
GO:0019901~protein kinase binding	2,13E-03
hsa05140:Leishmaniasis	2,37E-03
hsa04215:Apoptosis - multiple species	2,51E-03
hsa05132:Salmonella infection	2,51E-03
GO:0090200~positive regulation of release of cytochrome c from mitochondria	2,58E-03
R-HSA-373076~Class A/1 (Rhodopsin-like receptors)	2,66E-03
GO:0060754~positive regulation of mast cell chemotaxis	3,17E-03
hsa05224:Breast cancer	3,22E-03
hsa05220:Chronic myeloid leukemia	3,41E-03
GO:0001525~angiogenesis	3,44E-03
GO:0030335~positive regulation of cell migration	3,44E-03
hsa04912:GnRH signaling pathway	3,87E-03
GO:0043615~astrocyte cell migration	4,37E-03
hsa05164:Influenza A	4,52E-03
hsa05144:Malaria	4,65E-03
GO:1904707~positive regulation of vascular smooth muscle cell proliferation	5,70E-03
GO:0030198~extracellular matrix organization	5,82E-03
hsa04670:Leukocyte transendothelial migration	6,84E-03
GO:0002237~response to molecule of bacterial origin	7,53E-03
GO:0016301~kinase activity	8,36E-03
GO:0032526~response to retinoic acid	8,61E-03
R-HSA-195399~VEGF binds to VEGFR leading to receptor dimerization	1,16E-02
R-HSA-194313~VEGF ligand-receptor interactions	1,16E-02
R-HSA-8939211~ESR-mediated signaling	1,18E-02
R-HSA-9616222~Transcriptional regulation of granulopoiesis	1,18E-02
GO:0005518~collagen binding	1,26E-02
GO:0000079~regulation of cyclin-dependent protein serine/threonine kinase activity	1,46E-02
GO:0031334~positive regulation of protein complex assembly	1,46E-02
GO:2000045~regulation of G1/S transition of mitotic cell cycle	1,47E-02

Term	FDR
GO:0048246~macrophage chemotaxis	1,47E-02
GO:0001775~cell activation	1,47E-02
hsa04510:Focal adhesion	1,51E-02
R-HSA-111453~BH3-only proteins associate with and inactivate anti-	1,57E-02
apoptotic BCL-2 members	
GO:0030155~regulation of cell adhesion	1,57E-02
R-HSA-500792~GPCR ligand binding	1,58E-02
GO:0048661~positive regulation of smooth muscle cell proliferation	1,60E-02
GO:0043922~negative regulation by host of viral transcription	1,60E-02
GO:0038084~vascular endothelial growth factor signaling pathway	1,60E-02
hsa05143:African trypanosomiasis	1,67E-02
hsa01524:Platinum drug resistance	1,67E-02
R-HSA-75205~Dissolution of Fibrin Clot	1,80E-02
R-HSA-453279~Mitotic G1 phase and G1/S transition	1,80E-02
hsa05214:Glioma	1,92E-02
GO:1902230~negative regulation of intrinsic apoptotic signaling pathway	0.11E.00
in response to DNA damage	2,11E-02
hsa01521:EGFR tyrosine kinase inhibitor resistance	2,25E-02
hsa05212:Pancreatic cancer	2,25E-02
GO:0000082~G1/S transition of mitotic cell cycle	2,27E-02
GO:0000165~MAPK cascade	2,28E-02
GO:0005520~insulin-like growth factor binding	2,31E-02
GO:0044389~ubiquitin-like protein ligase binding	2,31E-02
hsa04672:Intestinal immune network for IgA production	2,55E-02
hsa05225:Hepatocellular carcinoma	2,78E-02
hsa04660:T cell receptor signaling pathway	2,78E-02
GO:0008233~peptidase activity	2,86E-02
GO:0044267~cellular protein metabolic process	2,89E-02
GO:0045893~positive regulation of transcription, DNA-templated	2,96E-02
R-HSA-109581~Apoptosis	2,96E-02
R-HSA-9006931~Signaling by Nuclear Receptors	2,96E-02
hsa05216:Thyroid cancer	3,03E-02
GO:0031012~extracellular matrix	3,07E-02
GO:0031093~platelet alpha granule lumen	3,07E-02
R-HSA-194138~Signaling by VEGF	3,10E-02
R-HSA-3700989~Transcriptional Regulation by TP53	3,31E-02
R-HSA-2022090~Assembly of collagen fibrils and other multimeric structures	3,31E-02

Term	FDR
R-HSA-109606~Intrinsic Pathway for Apoptosis	3,31E-02
GO:0034976~response to endoplasmic reticulum stress	3,54E-02
R-HSA-168643~Nucleotide-binding domain, leucine rich repeat containing receptor (NLR) signaling pathways	3,54E-02
GO:0070374~positive regulation of ERK1 and ERK2 cascade	3,73E-02
$R-HSA-8862803 {\sim} Deregulated CDK5 \ triggers \ multiple \ neurodegenerative$ pathways in Alzheimer's disease models	3,77E-02
R-HSA-8863678~Neurodegenerative Diseases	3,77E-02
GO:0008584~male gonad development	3,92E-02
R-HSA-5357801~Programmed Cell Death	4,27E-02
GO:0005788~endoplasmic reticulum lumen	4,40E-02
GO:0002548~monocyte chemotaxis	4,50E-02
GO:2001243~negative regulation of intrinsic apoptotic signaling pathway	4,50E-02
GO:0044344~cellular response to fibroblast growth factor stimulus	4,50E-02
R-HSA-9009391~Extra-nuclear estrogen signaling	4,56E-02
R-HSA-69206~G1/S Transition	4,56E-02
R-HSA-9734009~Defective Intrinsic Pathway for Apoptosis	4,56E-02
GO:0010971~positive regulation of G2/M transition of mitotic cell cycle FDR= False discovery rate	4,81E-02

 $\textbf{Supplementary table 8} \cdot \textbf{Drug-gene interactions for the 10 most significantly differentially expressed drugs of endotype 2.}$ 

Gene	Drug	Gene	Drug
MMP1	DOXYCYCLINE CALCIUM	PLAU	CISPLATIN
MMP1	COLLAGENASE CLOSTRIDIUM HISTOLYTICUM	PLAU	RETINOL
MMP1	RIBAVIRIN	PLAU	ESTRADIOL
MMP1	SIROLIMUS	PLAU	UROKINASE
MMP1	LEUPROLIDE ACETATE	PLAU	SARUPLASE
MMP1	PENTOSAN POLYSULFATE SODIUM	PLAU	SIROLIMUS
MMP1	TRIAMCINOLONE	PLAU	RAZOXANE
MMP1	LEFLUNOMIDE	PLAU	FILGRASTIM
MMP1	DOXYCYCLINE	PLAU	CARMUSTINE
MMP1	MEDROXYPROGESTERONE ACETATE	PLAU	VERAPAMIL
MMP1	HYDROCORTISONE	PLAU	HYDROCORTISONE
MMP1	LAMIVUDINE	MMP2	SIMVASTATIN
CXCL12	VINCRISTINE	MMP2	RAMIPRIL
CXCL12	ALEMTUZUMAB	MMP2	ACETAZOLAMIDE
CXCL12	PREDNISONE	MMP2	CYCLOSPORINE

Gene	Drug	Gene	Drug
CXCL12	CYCLOPHOSPHAMIDE	MMP2	BEVACIZUMAB
CXCL12	CHLORAMBUCIL	MMP2	STREPTOZOCIN
CXCL12	RITUXIMAB	MMP2	PRAVASTATIN
PLAU	PAPAVERINE	MMP2	PACLITAXEL
PLAU	AZACITIDINE	MMP2	ZILEUTON
PLAU	CALCITRIOL	MMP2	VINBLASTINE
PLAU	ALENDRONIC ACID	MMP2	FILGRASTIM
PLAU	DACARBAZINE	MMP2	LETROZOLE
PLAU	ZOLEDRONIC ACID	MMP2	DEFEROXAMINE
		CCL3	INFLIXIMAB

 $\textbf{Supplementary table 9} \ - \ \text{Patients demographics of the 21 metabolomic samples overlapping with cartilage endotypes} \ \text{as well as the 123 metabolomic samples measured in blood}.$ 

	overlapping sampl cartilage (N=21)	es with aged	with aged Total metabolite dataset (	
		N		N
Age (S.D.)	72.4(5.8)	21	69.3(9.2)	112
Females	14	21	78	115
Knee joints	11	21	59	115
BMI (S.D.)	28.1(3.2)	20	28.6(4.8)	106
JSN (S.D.)	4.3(1.7)	21	4.4(1.4)	62
Osteophyte	2.8(2.2)	21	3.9(2.2)	62
KL score	2.7(0.6)	18	3.0(0.7)	58

The demographics of the metabolomics datasets, the total dataset (n=123) has an overlap with cartilage data (n=21). JSN= joint space narrowing, Osteophyte= osteophyte score, KL score = Kellgren-Lawrence score, S.D. = standard deviation, N=sample size.

 $\textbf{Supplementary table 10} \ - \ \text{Linear model of BMI with independent variable Metabolomic endotypes of Figure 4.} \ Formula: \\ \text{Metabolomic endotypes} \ \sim \ \text{Age + Sex + BMI, A. of 20 metabolomic samples, overlapping with mRNA data and B, of 105 samples.}$ 

Α

Parameter	В	Std. Error	95% Wald Confidence Interval		Hypothesis Test		
			Lower	Upper	Wald Chi-Square	df	Sig.
(Intercept)	23,85	13,2	-2,03	49,73	3,26	1	0,07
Age	-0,27	0,12	-0,49	-0,04	5,15	1	0,02
[Sex=1]	0,02	1,1	-2,14	2,19	0	1	0,98
[Sex=2]	O <sup>a</sup>						
BMI	-0,17	0,2	-0,57	0,23	0,66	1	0,42
(Scale)	1						

Dependent Variable: Endotype\_Metabolomic, Model: (Intercept), Age, Sex, BMI, a.Set to zero because this parameter is redundant, N=20 (1 sample was excluded due to incomplete BMI data).

В

Parameter	В	Std. Error	95% Wald Confidence Interval		Std. Error 95% Wald Confidence Interval Hypothesis Test			
			Lower	Upper	Wald Chi-Square	df	Sig.	
(Intercept)	3,05	2,37	-1,58	7,69	1,67	1	0,2	
Age	-0,02	0,02	-0,07	0,03	0,74	1	0,39	
[Sex=1]	-1,04	0,44	-1,9	-0,18	5,62	1	0,02	
[Sex=2]	O <sup>a</sup>							
BMI	-0,05	0,05	-0,14	0,05	0,95	1	0,33	
(Scale)	1							

Dependent Variable: Endotype\_Metabolomic, Model: (Intercept), Age, Sex, BMI, a.Set to zero because this parameter is redundant, N=105 (17 sample were excluded due to incomplete BMI data).

 $\textbf{Supplementary table 11} \ - \ \text{General Estimation Equations of metabolites}, \ \text{showing all FDR significant metabolites}, \ \text{corrected for age, Sex and BMI in 20 samples. Formula: Metabolites} \ - \ \text{Metabolites} \ + \ \text{Age + Sex + BMI}.$ 

Metabolite	estimate	san.se	wald	FDR
Clinical_LDL_C	-1,92	0,16	141,25	8,94E-31
L_LDL_L	-1,96	0,17	125,52	1,23E-27
non_HDL_C	-1,82	0,17	113,79	3,04E-25
Total_C	-1,92	0,2	91,45	1,45E-20
Total_FC	-1,86	0,19	91,44	1,45E-20
Total_CE	-1,93	0,21	87,62	8,34E-20
S_LDL_L	-1,55	0,17	84,82	2,93E-19
ApoB	-1,69	0,18	84,52	3,00E-19
IDL_L	-2,04	0,22	84	3,47E-19
M_LDL_L	-1,62	0,2	69,22	6,99E-16

Metabolite	estimate	san.se	wald	FDR
Total_L	-1,58	0,21	57,83	1,63E-13
Total_PL	-1,77	0,28	41,01	7,96E-10
DHA	-1,71	0,32	28,53	4,48E-07
Sphingomyelins	-1,87	0,38	24,6	3,17E-06
Omega_3	-1,47	0,31	22,8	7,57E-06
XS_VLDL_L	-1,85	0,39	22,51	8,25E-06
SFA	-1,43	0,31	21,55	1,28E-05
Cholines	-1,82	0,4	21,1	1,53E-05
Phosphoglyc	-1,81	0,4	20,54	1,93E-05
VLDL_C	-1,2	0,27	20,4	1,98E-05
S_HDL_L	-1,45	0,32	20,11	2,19E-05
Phosphatidylc	-1,82	0,41	19,28	3,24E-05
PUFA	-1,4	0,32	19,16	3,29E-05
Total_FA	-1,28	0,31	16,99	9,86E-05
Omega_6	-1,24	0,31	16,11	1,51E-04
ApoA1	-1,5	0,41	13,37	6,18E-04
LA	-1,06	0,3	12,73	8,38E-04
M_HDL_L	-1,4	0,4	12,39	9,73E-04
HDL_C	-1,35	0,47	8,32	8,50E-03
M_VLDL_L	-0,62	0,22	7,49	0,0131
His	0,61	0,23	6,96	1,69E-02
S_VLDL_L	-0,83	0,32	6,5	2,13E-02
LDL_size	-0,49	0,19	6,42	2,15E-02
Phe	0,81	0,32	6,24	2,31E-02
Lactate	0,21	0,09	6,07	2,48E-02
VLDL_size	0,82	0,34	6	2,50E-02
MUFA	-0,74	0,31	5,82	2,63E-02
Pyruvate	0,66	0,27	5,84	2,63E-02
Unsaturation N=20	-0,79	0,36	4,86	4,43E-02

53

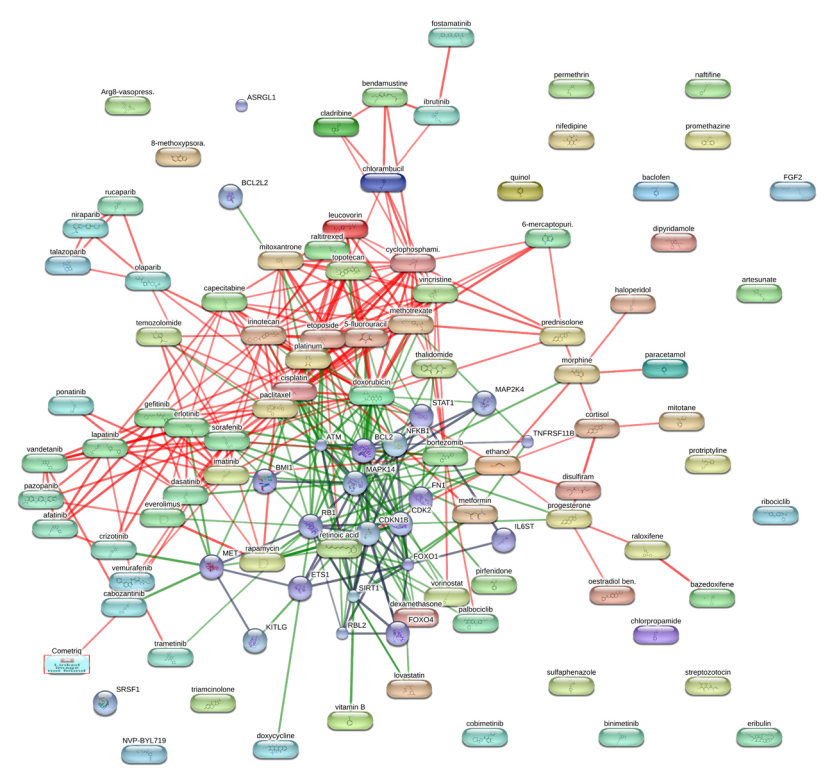


**Fig S1** - Drug-gene interactions of the 10 most significant differentially expressed genes for endotype 1. Green edges represent drug/gene interactions and red edges represent drug/drug interactions. Edges represent protein-protein associations, associations are meant to be specific and meaningful, i.e. proteins jointly contribute to a shared function; this does not necessarily mean they are physically binding each other. Edge Confidence: low (0.150) high (0.700) medium (0.400) highest (0.900)

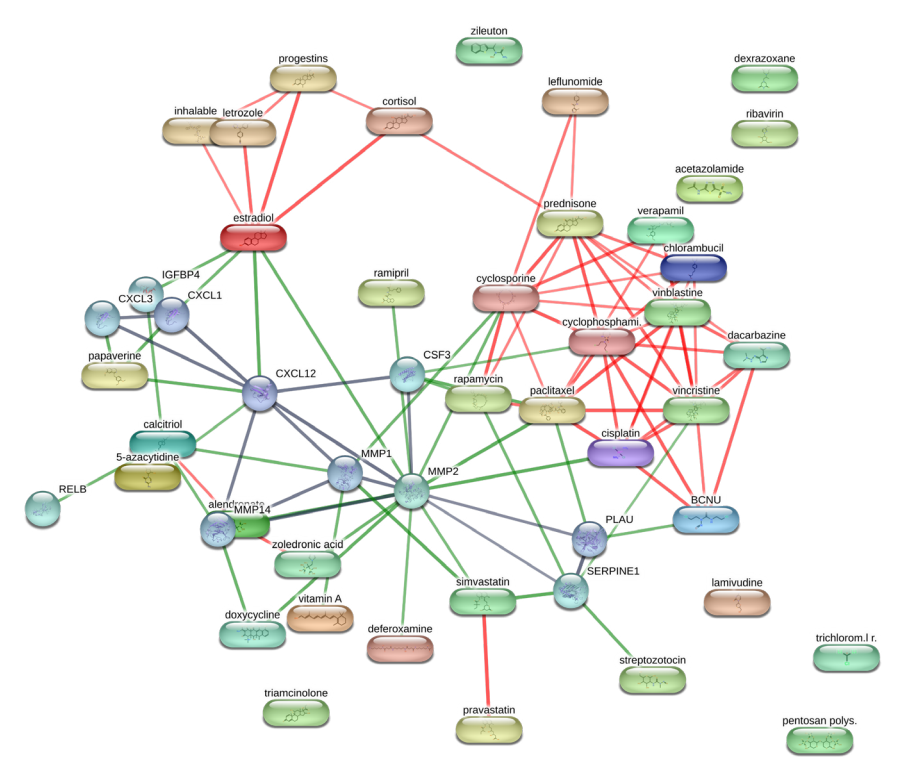


Fig S2 - Drug-gene interactions of the 10 most significant differentially expressed genes for endotype 2. Green edges represent drug/gene interactions and red edges represent drug/drug interactions. Edges represent protein-protein associations, associations are meant to be specific and meaningful, i.e. proteins jointly contribute to a shared function; this does not necessarily mean they are physically binding each other. Edge Confidence: low (0.150) high (0.700) medium (0.400) highest (0.900)

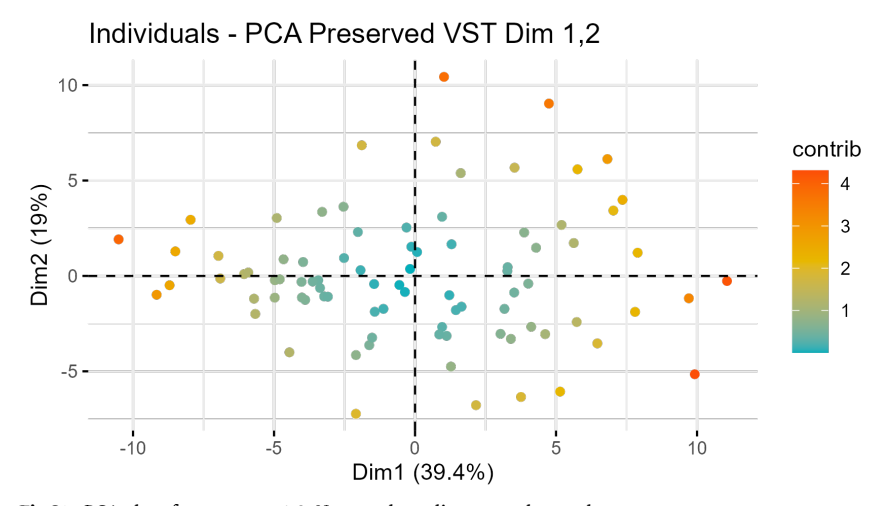


Fig S3 - PCA plot of component 1-2. No sample outliers were detected.